Gelatin Clay Hybrid Nanocomposites for Tissue Engineering Applications

by

Mohammad Towsif Hossain

B.Sc., Ahsanullah University of Science and Technology, Bangladesh, 2013

A THESIS SUBMITTED IN PARTIAL FULFILLMENT OF

THE REQUIREMENTS FOR THE DEGREE OF

MASTER OF APPLIED SCIENCE

in

THE COLLEGE OF GRADUATE STUDIES

(Civil Engineering)

THE UNIVERSITY OF BRITISH COLUMBIA

(Okanagan)

February 2018

The undersigned certify that they have read, and recommend to the College of Graduate Studies for acceptance, a thesis entitled:

Gelatin Clay Hybrid Nanocomposites for Tissue Engineering Applications

Submitted by Mohammad Towsif Hossain in partial fulfillment of the requirements of the degree of Master of Applied Science

Dr. Sumi Siddiqua, School of Engineering, UBCO
Supervisor, Professor (please print name and faculty/school above the line)

Dr. Keekyoung Kim, School of Engineering, UBCO
Co-supervisor, Professor (please print name and faculty/school in the line above)

Dr. Sunny Li, School of Engineering, UBCO
Supervisory Committee Member, Professor (please print name and faculty/school in the line above)

Dr. Chen Feng, School of Engineering, UBCO
University Examiner, Professor (please print name and faculty/school in the line above)

External Examiner, Professor (please print name and university in the line above)

February 02, 2018
(Date submitted to Grad Studies)

Abstract

Recent trends promote the replacement of synthetic polymer based hydrogel composites with different bio-polymer based composite due to superior biocompatibility and biodegradability. Again, some tissue engineering applications e.g. osteogenic diseases, stiff bio-polymer composite is required. Although, bone has splendid ability to heal itself after injury, there is still a space left to accelerate the healing process for non-union injuries. To address this problem, a novel gelatin based bio-nanocomposite material had been developed using ceramic particles found in clay minerals. Three different types of materials such as micro bentonite, nanosilica, and nanobentonite have been used in various concentration with gelatin hydrogel to increase its toughness. Micro bentonite did not interact with hydrogel chain whereas it was proved to be cell viable. Subsequently, nanosilica did increase the compressibility of the polymer but it was not compatible with the cells. Afterwards, nanobentonite was introduced. Nanobentonite is a smectite shaped ultra-thin nanomaterial. The nanobentonite was crosslinked with the gelatin hydrogel covalently to produce tunable physical and mechanical properties. Small amount of covalently bonded nanocomposite increased the elastic modulus of the gel by 6 folds and tensile stress by 10 folds. The nanoparticles also enhanced the pore size of the hydrogels which promoted the exchange of biomolecules in the matrices. The nanocomposite also amplified the cell adhesion, proliferation, and growth of NIH 3T3 fibroblast cells compared with the pristine gelatin hydrogel. Overall, the results of the nanocomposite showed promising improvement in terms of stiffness, porosity, cell viability which play vital role in the treatment of non-union bone defects.

Lay Summary

Many people suffer from bone loss after a certain age. Also, some people suffer from non-union bone defects due to accidents. A general approach is to surgically fix the problem, however, most of the time, the fractured bone does not set properly. Scientists are now trying to solve this problem through a noninvasive approach. Biodegradable and cell viable material, that can resemble the environment of the bone tissue can be used in the place of fracture via injection instead of critical surgery. The artificial biomaterial encourages the stem cells to grow on the fractured bone and heal the bone properly. In this study, a novel biomaterial was fabricated with proper micro-environment and strength of the bone which has the potential to mitigate the problem associated with bone decay as well as fractured bone.

Preface

The studies presented in this thesis are the original work of the author. The research was conducted under the supervision of Dr. Sumi Siddiqua and Dr. Keekyoung Kim at the Integrated Bio-Micro/Nanotechnology Laboratory in the School of Engineering at UBC Okanagan Campus.

Parts of the thesis are going to be published in the following journals:

1. A version of chapter 4 is going to be submitted in the journal of *Applied Clay Science*. M.T. Hossain, K. Saktivel, S. Siddiqua, and K. Kim, "Reinforcing GelMA Hydrogel with Nanobentonite for Regenerative Bone Tissue Scaffolds" 2018.
2. A version of chapter 2 is going to be submitted in the journal of *Biotechnology Advances*. M.T. Hossain, K. Saktivel, S. Siddiqua, and K. Kim, "Properties and biomedical applications of gelatin methacrylate (GelMA) hydrogels with nanoparticles" 2018.
3. Chapter 3 as a technical note is going to be published in the journal of *Applied Clay Science.*

Table of Contents

Abstract ..... **iii**

Lay Summary ..... **iv**

Preface ..... **v**

Table of Contents ..... **vi**

List of Tables ..... **ix**

List of Figures ..... **x**

List of Abbreviations ..... **xv**

Acknowledgements ..... **xvii**

Dedication ..... **xviii**

Chapter 1: Introduction **1**

1.1 Tissue Engineering 1

1.2 Hydrogels 4

1.3 Nanoparticles 7

1.4 Nanocomposite Hydrogels 9

1.5 Research Objective 13

1.6 Chapter Outline 14

Chapter 2: Gelatin Methacrylate Hydrogels **16**

2.1 GelMA Hydrogel 17

2.2 GelMA Synthesis 18

2.3 Physical Properties of GelMA 19

2.4 GelMA with Nanoparticles 21

2.4.1 GelMA with Carbon Nanoparticles 21

2.4.2 GelMA with Graphene Nanoparticles 23
2.4.3 Inorganic Nanoparticles 24
2.4.4 Metal Oxide 25
2.5 Summary 27
Chapter 3: GelMA with Micro Bentonite and Nanosilica 28
3.1 Characterization of Particles 28
3.1.1 Micro Bentonite 28
3.1.2 Nanosilica 29
3.2 Crosslinking of GelMA Composites 30
3.2.1 GelMA with Micro Bentonite 30
3.2.2 GelMA with Nanosilica 31
3.3 Mechanical Characterization of GelMA Composites 35
3.3.1 GelMA with Micro Bentonite 35
3.3.2 GelMA with Nanosilica 37
3.4 Cell Viability of GelMA Composites 39
3.4.1 GelMA with Micro Bentonite 39
3.4.2 GelMA with Nanosilica 41
3.5 Summary 43
Chapter 4: Crosslinkable and Cell Viable GelMA with Nanobentonite 45
4.1 Introduction 45
4.2 Materials 48
4.2.1 Nanobentonite 48
4.2.2 Gelatin Methacrylate (GelMA) 50

4.2.3 Fabrication of Nanocomposites (GelMA with nanobentonite) 50
4.3 Characterization of Physical Properties 51
4.4 Assessment of Cell Viability 52
4.5 Statistical analysis 53
4.6 Results and Discussion 53
4.6.1 Crosslinking Nanobentonite with GelMA 54
4.6.2 Enhancing Mechanical Stiffness 58
4.6.3 Nanobentonite enhanced cell adhesion and proliferation 60
4.7 Summary 62
Chapter 5: Conclusion 64
5.1 Conclusions 64
5.2 Major Contributions 65
5.3 Future Work 65
5.3.1 *In Vivo* Studies 66
5.3.2 Architecture of Tissue Scaffolds 66
References 68

List of Tables

Table 2.1 Relationship between different physical properties of GelMA. 20

Table 2.2 Different aspects of CNTs-GelMA hybrid hydrogels..... 22

Table 2.3 Different aspects of Graphene-GelMA hydrogel..... 23

Table 2.4 Different aspects of nanosilicates-GelMA hydrogel. 24

Table 2.5 Different aspects of metal nanoparticles-GelMA hydrogel. 26

Table 3.1 Mineralogical composition of bentonite in micro scale..... 29

Table 3.2 Chemical composition of bentonite and bentonite nanoparticles. 29

List of Figures

Figure 1.1 A typical workflow of tissue engineering using hydrogel scaffolds (adapted from [4]). 2

Figure 1.2 A typical bone tissue transplantation using hydrogel graft (adapted from [9]). 4

Figure 1.3 Resemblance between hydrogel and natural tissue. (A) Representative Hydrogel scaffolds under SEM. (B) ECM of intramuscular connective tissue after removal of skeleton muscle protein under SEM (adapted from [27]). 6

Figure 1.4 Natural tissue variation induces differentiation marker expression in stem cells [33]. (A) ECM elasticity of different tissues. (B) Collagen based gel resembling the microenvironment of various tissues. (C) Stem cells showing different markers to grow into different cells based on the elasticity of gel. 7

Figure 1.5 A typical mechanical process for nanobentonite extraction from Wyoming clay (adapted from [58]). 9

Figure 1.6 A schematic of the formation of the nanocomposites hydrogels with various nanoparticles (adapted from [60]). 11

Figure 2.1 (A) Publication related to hydrogel. (B) Publication related to nanocomposite hydrogel (Adapted from [59]). 16

Figure 2.2 General process of GelMA hydrogel synthesis. 19

Figure 3.1 Particle size analysis for micro Bentonite under SEM (Tescan Mira3 XMU Field Emission Scanning Electron Microscope), bar represents 10 µm. 28

Figure 3.2 SEM image of nanosilica. Scale bar = 2 µm. 29

Figure 3.3 Represantative crosslinked samples around 1 cm in diameter of (A) pristine GelMA and (B) GelMA with micro bentonite. 30

Figure 3.4 Micro structure of GelMA and hybrid GelMA after adding micro bentonite. (A) 5% GelMA. Scale bar = 20 µm. (B) 5% GelMA with 0.2% micro bentonite. Scale bar = 50 µm (C) 5% GelMA with 0.5% micro bentonite. Scale bar = 50 µm. 31

Figure 3.5 Represantative crosslinked samples around 1 cm in diameter of (A) pristine GelMA and (B) GelMA with nanosilica. 32

Figure 3.6 EDS analysis of GelMA and hybrid GelMA after adding nanosilica. (A) EDS of nanosilica. (B) EDS of GelMA hydrogel. (C) EDS of GelMA hydrogel with nanosilica. 33

Figure 3.7 Micro structure of GelMA and hybrid GelMA after adding nanosilica. (A) 5% GelMA, scale bar = 20 µm. (B) 5% GelMA with 0.2% nanosilica, scale bar = 50 µm. (C) 5% GelMA with 0.5% nano silica, scale bar = 20 µm. (D) 5% GelMA with 1% nanosilica, scale bar = 20 µm. 34

Figure 3.8 FT-IR spectra of hybrid hydrogel. (A) Silica nanoparticles with Si-O-Si peak. (B) Pristine GelMA with amides peaks. (C) Hybrid nanosilica GelMA with both Si-O-Si and amides peaks. 35

Figure 3.9 Characterization of the mechanical properties of micro bentonite hybrid GelMA: Determining the elastic modulus of 5% GelMA and various concentration of micro bentonite with GelMA (n=5). 36

Figure 3.10 Characterization of the mechanical properties of nanosilica hybrid GelMA: Determining the elastic modulus of 5% GelMA and various concentration of nanosilica with GelMA (*p<0.05, n=5). 37

Figure 3.11 Effect of nanosilica on mass swelling ratio was investigated. Mass swelling ratio of 5% pristine GelMA and hybrid GelMA with various concentration of nanosilica (n=5). 38

Figure 3.12 2D bright view image 3T3 cells on GelMA and different concentrations of micro bentonite with GelMA at day 3. (A) 5% GelMA with 0% micro bentonite. (B) 5% GelMA with 0.1% micro bentonite. (C) 5% GelMA with 0.2% micro bentonite. (D) 5% GelMA with 0.5% micro bentonite. (E) 5% GelMA and 1.0% micro bentonite. Scale bar = 50 µm. 40

Figure 3.13 Interaction of 3T3 fibroblast cells with various concentration of micro bentonite at day 1. (A) 0% micro bentonite. (B) 0.1% micro bentonite (C) 0.2% micro bentonite. (D) 0.5% micro bentonite. (E) 1.0% micro bentonite. Scale bar = 50 µm. 41

Figure 3.14 2D bright view image 3T3 cells on GelMA and different concentrations of micro bentonite with GelMA at day 3. (A) 5% GelMA with 0% nanosilica, scale bar = 50 µm. (B) 5% GelMA with 0.2% nanosilica., scale bar = 50 µm. (C) 5% GelMA with 0.5% nanosilica, scale bar = 50 µm. (D) 5% GelMA with 1% nanosilica, scale bar = 50 µm. 42

Figure 3.15 Interaction of 3T3 fibroblast cells with various concentration of nanosilica at day 1. (A) 0% nanosilica, scale bar = 50 µm. (B) 0.2% nanosilica, scale

bar = 50 µm. (C) 0.5% nanosilica, scale bar = 50 µm. (D) 1% nanosilica, scale bar = 50 µm. 43

Figure 4.1 Schematic of the formation of GelMA and hybrid GelMA. (A) Gelatin Methacrylate. (B) GelMA hydrogel. and (C) nanocomposite i.e. nanobentonite with GelMA hydrogel. 53

Figure 4.2 SEM image of nanobentonite. Scale bar = 500 nm. 54

Figure 4.3 FT-IR spectra of hybrid hydrogel. (A) Bentonite nanoparticles with Si-O-Si peak. (B) Pristine GelMA with amides peaks. (C) Hybrid nanobentonite GelMA with both Si-O-Si and amides peaks. 55

Figure 4.4 Effect of nanobentonite on mass swelling ratio was investigated. Mass swelling ratio of 7% pristine GelMA and hybrid GelMA with various concentration of nanobentonite (***$p<0.001$, n=5). 56

Figure 4.5 Micro structure of GelMA and hybrid GelMA after adding nanobentonite. (A) 7% GelMA, scale bar = 20 µm. (B) 7% GelMA with 0.1% nanobentonite, scale bar = 20 µm. (C) 7% GelMA with 0.2% nanobentonite, scale bar = 50 µm. (D) 5% GelMA with 0.5% nanobentonite, scale bar = 50 µm. 57

Figure 4.6 EDS of hybrid hydrogel. (A) Bentonite nanoparticles with Al, Na, Si, Mg, and Ca peaks. (B) Pristine GelMA with N, C, O, Cl, Na peaks. (C) Hybrid nanobentonite GelMA with elements both from nanobentonite and GelMA hydrogel. 58

Figure 4.7 Physical Testing of Hybrid GelMA with Nanobentonite. (A) 7% pristine GelMA. (B) 7% GelMA with 0.1% nanobentonite. (C) 7% GelMA with 0.2% nanobentonite. (D) 7% GelMA with 0.5% nanobentonite. 59

Figure 4.8 Characterization of the mechanical properties of nanobentonite hybrid GelMA: Determining the elastic modulus of 7% GelMA and various concentration of nanobentonite with GelMA (*p<0.05, ***p<0.001, n=5). 59

Figure 4.9 Characterization of the mechanical properties of nanobentonite hybrid GelMA: Determining the Strain-stress curve of 7% GelMA and various concentration of nanobentonite with GelMA..... 60

Figure 4.10 2D image of live/dead assay at day 5. (A) pristine 7% GelMA hydrogel. (B) 0.1% nanobentonite crosslinked with GelMA. and (C) 0.5% nanobentonite crosslinked with GelMA. Scale for all the images = 200 µm. 61

Figure 4.11 Cell viability at day 5 of pristine GelMA and nanobentonite crosslinked with GelMA, n=5, *p<0.05. 62

List of Abbreviations

ECM	Extracellular matrix
LDHs	Layered double hydroxides
TMDs	Transition metal dichalcogenides
TMOs	Transition metal oxides
PTT	Photo thermal therapy
PDT	Photodynamic therapy
RGD	Arginine-glycine-aspartic acid
EDS	Energy dispersive spectroscopy
UV	Ultra violet light
FT-IR	Fourier transform infrared spectra
PBS	Phosphorus buffer solution
NIP	Nano iron particles
nZVI	Nano zero-valent iron
CNTs	Carbon nanotubes
GO	Graphite oxide
GPO	Graphene peroxide
HPE	Hyperbranched poly amineester
HA	Hydroxyapatite
PEG	Poly ethylene glycol
SEM	Scanning electron microscope
XRD	X-ray Powder Diffraction
XRF	X-ray Fluorescence

MMP	Metalloproteinase
MA	Methacrylic anhydride

Acknowledgements

First, I would like to express my gratitude to my supervisors, Dr. Sumi Siddiqua and Dr. Keekyoung Kim, for their guidance to study in the University of British Columbia, Okanagan. Without their continuous support, expertise and motivation, this thesis would not become in reality. I would also like to thank my committee member, Dr. Sunny Li for his crucial suggestion on my research projects, and my external examiner Dr. Chen Feng, for taking the time to read and critique my thesis.

I also must acknowledge Dr. Deborah Roberts for providing her lab facilities and training for the instrumentations.

I am also grateful to all past and present members of the Integrated Bio-Micro/Nanotechnology and Geotechnical Laboratory for all the valuable discussions and for assisting me to finish the experiments, the staff members of the School of Engineering, especially Michelle Dawn Tofteland, for helping me prepare my researches. I also want to remember David Arkinstall for helping with the imaging process.

I also like to thank NSERC, DG, and work study program to provide fund to finish the research.

I would like to express my greatest gratitude to my parents, spouse, brother and sister, nephews, and relatives without their unconditional love, caring and passions I will not be able to complete the thesis.

Dedicated to

My Father, MD. Towhid Hossain

My Mother, Ferdous Ara

And Shila

Chapter 1: Introduction

Researchers have been investigating the traits and gaining significant development in artificial biomaterials to treat the loss, defects, and failure of the bone tissues for the last few years [1]. Conventional autograft and allograft are promising methods to treat osteogenic diseases but both these methods are compromised with the inherited problems of finding the proper donor sites and dangerous transmissible diseases [1]. Therefore, scientists have been trying to craft artificial materials that can mimic the extra cellular matrix (ECM) of bone tissue using polymers, ceramics, and metals. Different types of biopolymers are now in use to create bone tissue environment that passed the laboratory stage and held in clinical trial. However, the present biomaterials exceed low mechanical properties and show limited structural integrity required to exhibit strong ECM to promote osteogenic cell proliferation and differentiation [2]. To address these issues, introduction of nanobentonite (nanoscale) into the network of collagen based biomaterial has been assessed in this study which has showed promise in strengthening the graft imitating bone tissue.

1.1 Tissue Engineering

In tissue engineering, the targeted cells are infused in biomaterials to build a temporary scaffolds to obtain a proper ECM for artificial tissues using mainly two different methods namely top-down or bottom-up methods [3]. Figure 1.1 shows the common tissue engineering culture, replacement, and implant procedure. Cells are cultured homogeneously in the graft of biomaterials to mimic the mimic the artificial tissues in top-down method. Regardless of how the cells are seeded, in top-down method, it is very difficult to control the ECM microenvironments due to the inhomogeneity of the matrix [3]. Therefore, having the proper

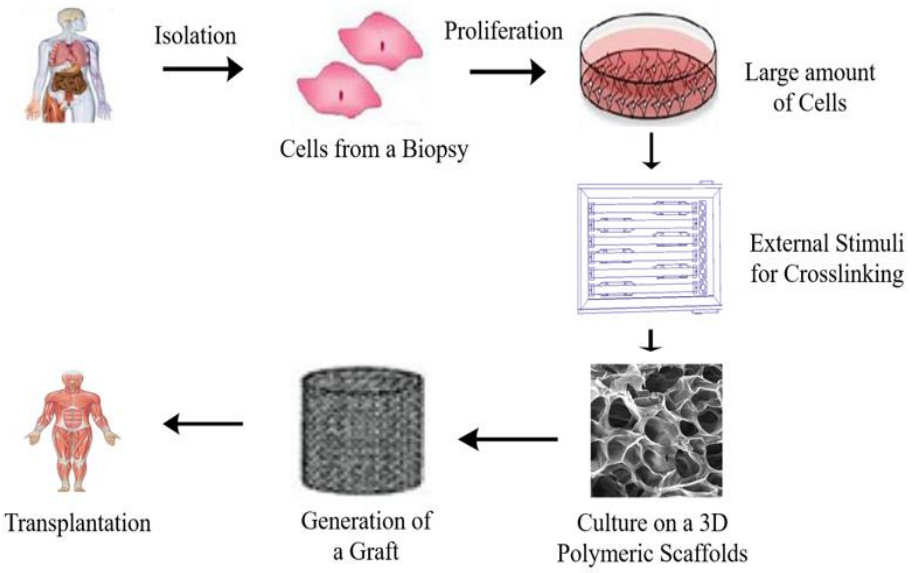

Figure 1.1 A typical workflow of tissue engineering using hydrogel scaffolds (adapted from [4]**).**

ECM is a foremost specification for cells to grow on them to build tissue like structure. In contrast, brick-by-brick and layer-by-layer method using microfabrication is being used to build up tissues in bottom-up method. In this process, the distribution of the cells can be controlled better at micrometer scale and the functionality of the tissue scaffolds has been improved significantly [5]. Different methods including microengineered organ-on-a-chip platforms to imitate the tissue function in vitro [6], high yield rate differentiation of stem cells [7], and complex heterogenous tissues [8] are the most well investigated approaches in the bottom-up method.

The main objective of the study is concentrated to design a biomaterial that can promote osteogenic cells growth and proliferation at place of need. Therefore, the study of the bone's properties is necessary. The bone is a hierarchical structure of the body primarily comprised of bioceramics and complicated biopolymer (collagen). Bone provides the structural

arrangement of the body, keeps the internal organs such as heart, lungs, and brain safe [9]. The loss or dysfunction of bone tissue goes together with trauma, injury and results significant morbidity and other socio-economic issues. With the advancement of nanotechnologies, along with changes of patient demographics, it has become imperative for new, robust and more reliable osteogenic tissue regeneration strategies [10]. Thus, the emerging new approaches attempt to find innovative scaffolds, harness stem cells, and other biological factors for the enhancement of bone formation to improve the quality of the life for an ageing population. Depending on the clinical scenario, bone tissue engineering tends to solve the problems associated with fractures and arthrodesis, osteochondral defects, and bone defects [10]. For example, a tibial atrophic non-union [11], [12] needs stimulation to heal fracture [13], [14] whereas segmental bone defects require vascularized bone line structure which enables to integrate with the surrounding ECM microenvironments [15]–[20]. To address this issues several biomaterials including Poly(methyl methacrylate), polyglycolic acid, polyvinylpyrrolidone, poly(propylene fumarate), polydopamine, polyvinyl alcohol, polycaprolactone, collagen, chitin, chitosan, and alginate are in use to make grafts which accelerate the progression of particular stem cells [21], [22]. As the synthetic polymers exhibit unwanted byproducts while degradation, researchers are more interested in natural polymers with nanomaterials to graft skeletal tissues for suitable biocompatibility and biodegradability [9]. A general sketch of the bone graft procedure is presented in figure 1.2.

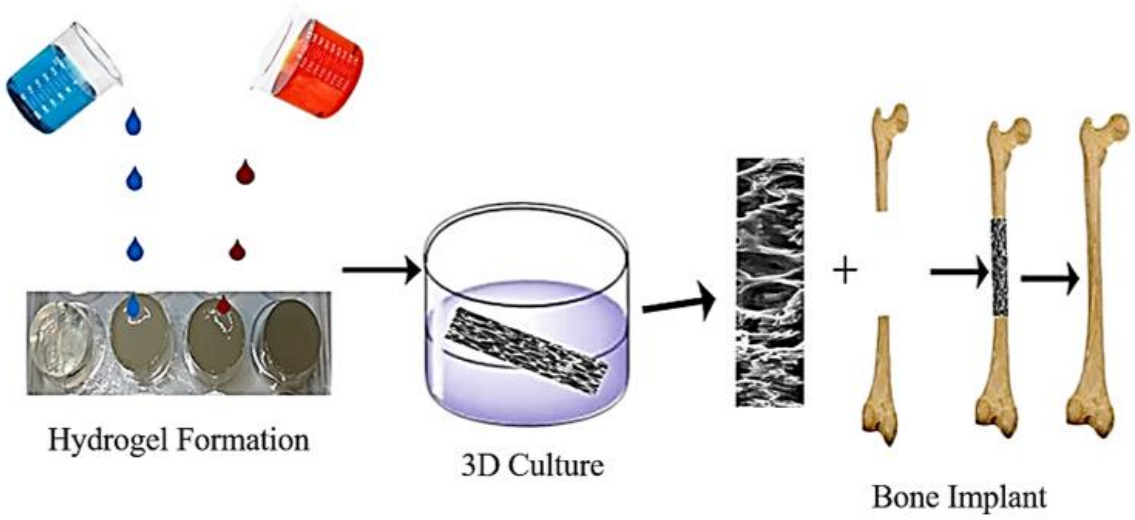

Figure 1.2 A typical bone tissue transplantation using hydrogel graft (adapted from [9]**).**

1.2 Hydrogels

Hydrogels are the most commonly used biomaterials for tissue engineering due its nature to mimic the *In Vivo* environments of cells [23]. Commonly, there are two types of hydrogels considering the design i.e. natural polymer-based hydrogels and synthetic polymer-based hydrogels [24]. Natural hydrogels constitute of gelatin, collagen, laminin, and fibronectin which are found in ECM components and the alginate, chitosan, and silk fibroin are the synthetic polymers used in design of synthetic hydrogels. The interaction between cells and natural hydrogels are well documented [24]. Whereas, synthetic hydrogels are processed through chemical synthesis therefore their mechanical and chemical properties are more controllable [25]. But, the interaction between cells and synthetic hydrogels are not well investigated systematically [24]. However, natural hydrogels and synthetic hydrogels have both been used in tissue engineering research [8]. Hydrogels in its pre-polymer form stay in liquid state before solidification. Solidification of the pre-polymer solution happens in the

presence of external factors such as temperature, chemicals, and illumination [26]. The solidification process is called the crosslinking where polymers make chains of network. Among other crosslinking, (such as thermal and chemical) photo crosslinking has become the most popular method in the recent years [24]. Because, photo crosslinking occurs (usually from several seconds to a few minutes) without affecting the microstructure of the fabricated structures in situ and maintain a minimal heat production suitable for cell physiology [28]. The optimal temperate and invasion caused by photo crosslinking is suitable for giving the accurate shape to the biomaterial which can conform to functional tissue. The crosslinked hydrogels provide a solid 3D cellular microenvironment suitable for cell growth and proliferation. In addition, hydrogels must have sufficient mechanical properties to offer cells growth and proliferation [29]. Strain, shear stress, elastic modulus, and mass swelling ratio determine the mechanical properties of hydrogels. Soft tissues like cartilage and skin tissues require enough mechanical strength to function on the hydrogel scaffold [30]. Also, it is essential for hydrogels to blend in with the surrounding *in vivo* so that the scaffolds can be degraded and integrated in time [31]. However, the hydrogel used for the study is a gelatin based hydrogel having good biodegradability and biocompatibility but it is a "soft" gel [32]. But, its rigidity can be increased by increasing the concentration of the crosslinker at the cost of low biocompatibility [34], [35]. Therefore, maintaining the proper rigidity and toughness of the hydrogel without affecting the biocompatibility is the challenge for biomedical engineers.

If freeze-dried hydrogels are characterized under SEM most hydrogel polymers resemble the structure of human tissue ECM. For example, SEM image of hydrogel and intravascular tissue of connective tissue upon the removal of the protein is shown in figure 1.3. Additionally, the elasticity of the ECM regulates the stem cell differentiation [33]. Stem cells show different

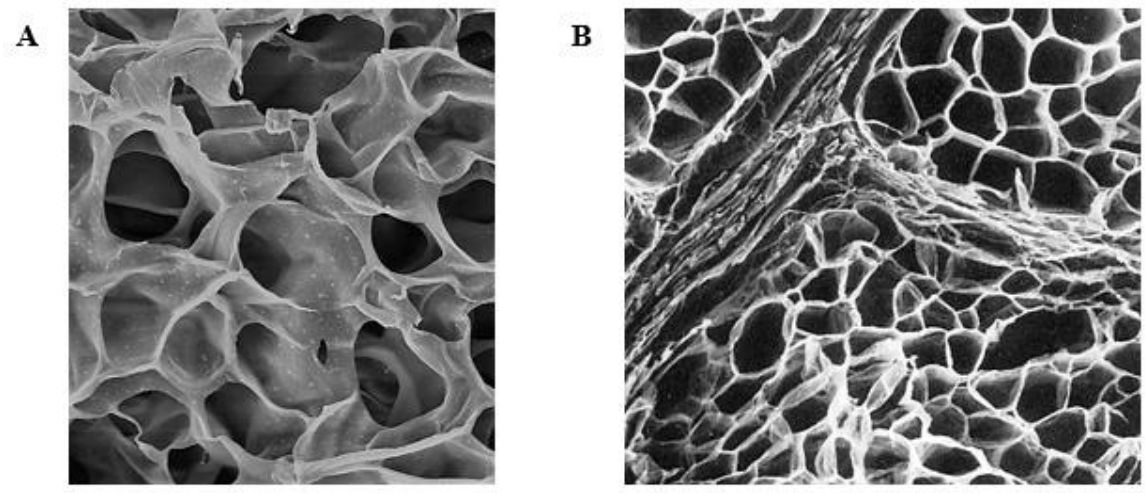

Figure 1.3 Resemblance between hydrogel and natural tissue. (A) Representative Hydrogel scaffolds under SEM. (B) ECM of intramuscular connective tissue after removal of skeleton muscle protein under SEM (adapted from [27]**).**

markers for different cells when the microenvironment is controlled mechanically. The elastic modulus of the different tissues from blood to bone is showed and in figure 1.4 and the stem cells grow into different cells due to the different elasticity in the microenvironment. Therefore, stem cells to differentiate into osteogenic tissue, the elasticity of the microenvironment needs to be more than 30 kPa. So, the design of hydrogel/hybrid hydrogel should be in a way that can mimic this microenvironment.

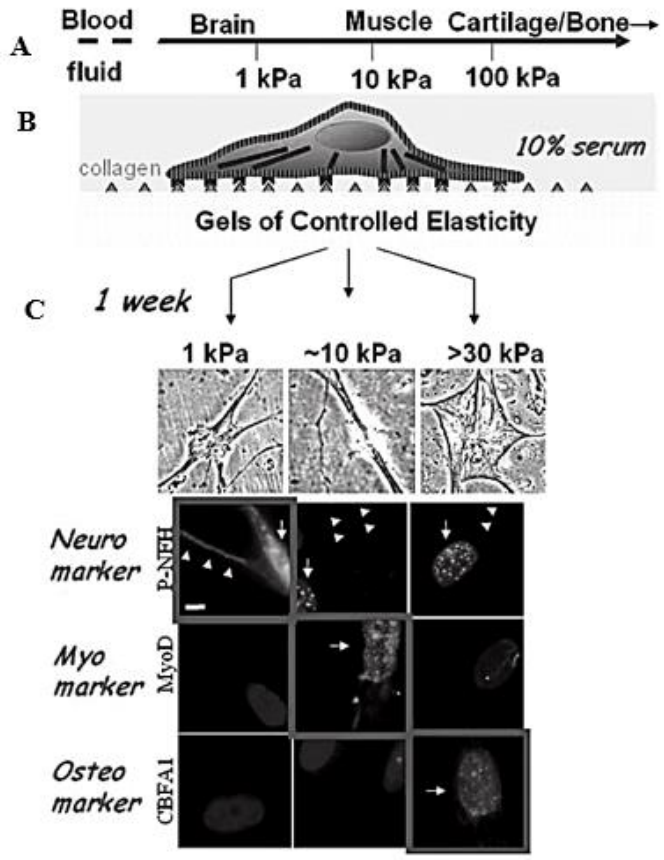

Figure 1.4 Natural tissue variation induces differentiation marker expression in stem cells [33]**. (A) ECM elasticity of different tissues. (B) Collagen based gel resembling the microenvironment of various tissues. (C) Stem cells showing different markers to grow into different cells based on the elasticity of gel.**

1.3 Nanoparticles

By definition, a particle is said to be nano if at least one of its dimension is less than 100 nm [36],[37]. Many novel materials have been developed using the unique properties of nanoparticles which are different from their natural state. The large surface to volume ratio of nanoparticles gives its unique characteristics as they can radically improve the catalytic process among materials [38]. Nanoparticles are in biomedical engineering commonly used with hydrogels to make nanocomposites to exhibit necessary features for different applications. Nanocomposites hydrogels have the potential to work as a graft for tissue engineering as well

as bio-fillers [39]. In case of drug delivery, chitosan hydrogel with montmorillonite has been used to investigate vitamin B-12 release under electro-stimulation [40] and hydrotalcite and iron nanoparticles have been used with various hydrogels to investigate sol-gel interaction with vitamin B-2 and other drugs [41]–[45]. Nanoparticles meshed with hydrogel scaffolds are widely used in 3D bioprinting to produce artificial tissue and organ. Carbon nanotubes [46], [47], hectorite clay [48], hydroxyapatite (HA) [49]–[51], bio-ceramic nanoparticles [52], [53], bioactive glass nanoparticles [54], laponite [55], silver nanoparticles [56], nano ZnO [57] are some of the nanoparticles, researchers have been investigating by incorporating with various hydrogels for different applications of tissue engineering.

In this study, bentonite nanoparticles have been used as the reinforcement agent for the hydrogel. Bentonite nanoparticles are categorized as an improved geotechnical material and it was produced in the Geotechnical Lab at University of British Columbia, Okanagan. Sarkar et al., described the mechanical process of artificial production of sodium rich bentonite nanoparticles from Wyoming bentonite [58]. In short, Wyoming bentonite clay was placed in planetary ball mill (pulverisette 7) to pulverize the coarse particles. An aqueous solution was made of pulverized clay and ultra-sonication probe was used to disperse the particles and centrifugation was used to settle down the large particles. Finally, the upper layer of the solution with nanoparticles were collected and filtered to obtain nanobentonite. A schematic of the mechanical process of obtaining nanobentonite from Wyoming bentonite clay is shown in figure 1.5.

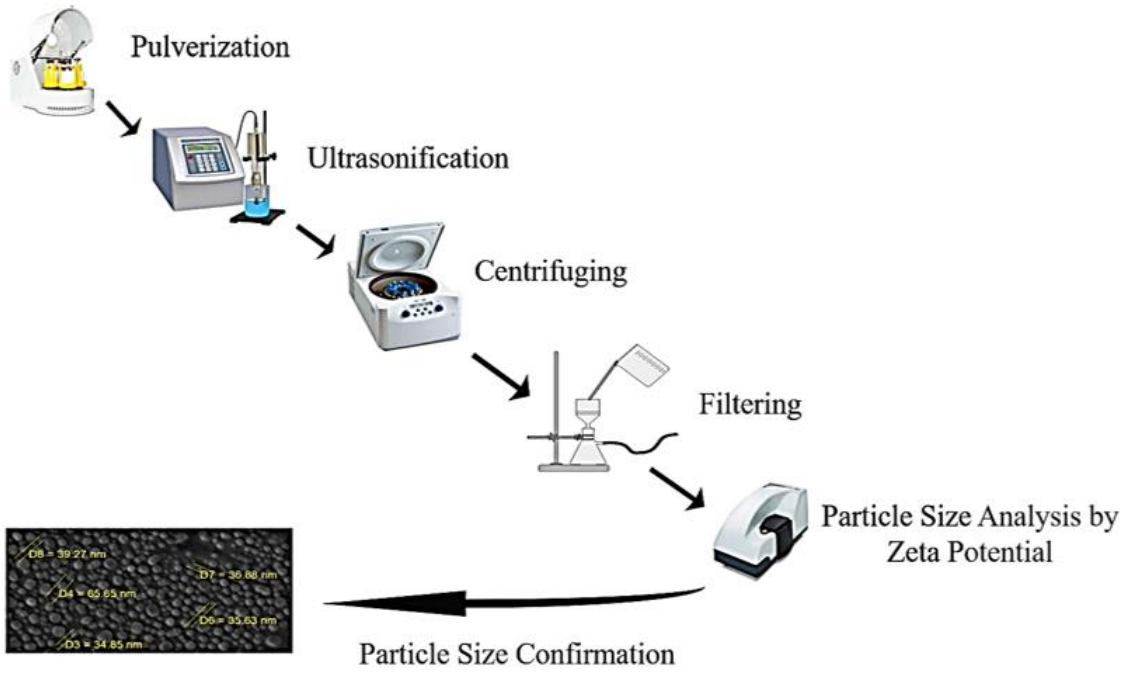

Figure 1.5 A typical mechanical process for nanobentonite extraction from Wyoming clay (adapted from [58]**).**

1.4 Nanocomposite Hydrogels

When hydrated polymeric networks are crosslinked with each other with nanoparticles or nanostructures either physically or covalently to form polymeric chains are called nanocomposite hydrogels, also known as hybrid hydrogels [59]. With time, new applications for hydrogels have emerged, therefore, multifunctionality and dynamic interactions between polymeric chains and cellular environments are required for applications like stem cell engineering, immunomodulation, cellular and molecular therapies, and cancer research [61], [62]. Thus, hydrogels need to be customized to meet the challenges of the trending biomedical engineering using the advancement in the field of polymer chemistry, nanofabrication technologies, and biomolecular engineering [63]. Although nanocomposites have numerous applications in electrical, mechanical, civil, and textile engineering, biomedical engineering,

biomedical engineering focuses in regenerative medicine, drug delivery, biosensors, and bioactuators which involve multifunctional nanocomposites hydrogels. Different types of nanoparticles harmless to human body are in use to incorporate with hydrogels and those are carbon-based nanomaterials (carbon nanotubes (CNTs), graphene, nano-diamonds), polymeric nanoparticles (polymer nanoparticles, dendrimers, hyperbranched polyesters), inorganic/ceramic nanoparticles (HA, silica, silicates, calcium phosphate), and metal/metal-oxide nanoparticles (gold, silver, iron-oxide) are combined with the polymeric network to obtain nanocomposite hydrogels. These nanoparticles are impregnated with various types of hydrogels physically or covalently to interact with the polymeric chains, and result in exhibiting novel properties of the nanocomposite network [64], [65], [66]. Tampering the properties of hydrogels with nanoparticles to our desire has unlocked the enormous possibilities in developing advanced biomaterials for various biomedical and biotechnological applications [67], [68]. Schematic of the formation of the nanocomposites hydrogels with various nanoparticles are shown in figure 1.6.

Among others Carbon-based nanomaterials such as CNTs, graphene, buckminsterfullerene (C60), and nanodiamonds are being extensively studied for the potential applications in biomedical engineering [69], [64]. Both CNTs- or graphene-based nanocomposite hydrogels have been used as actuators, conductive tapes, biosensors, tissue engineering scaffolds, drug delivery systems, and biomedical devices [70], [64]. Nerve, muscle, and cardiac tissues are compatible with CNTs based hydrogels due to their high electrical conductivity [59]. Multi-wall CNTs coated with gelatin hydrogels have the ability to increase the spontaneous beating rate cardiomyocytes [71]. Multiwall CNTs also responsible for strong interaction between gel and different proteins which can be used in drug delivery,

and biosensing [72]. Hydrogels reinforced with stabilized graphene i.e. graphite oxide (GO) play as an actuator which can bend, stretch and twist when subjected to different radiation intensities [73]. Functionalized graphene peroxide (GPO) has enhanced the mechanical stiffness of hydrogels required for cardiac and osteogenic tissue engineering [74].

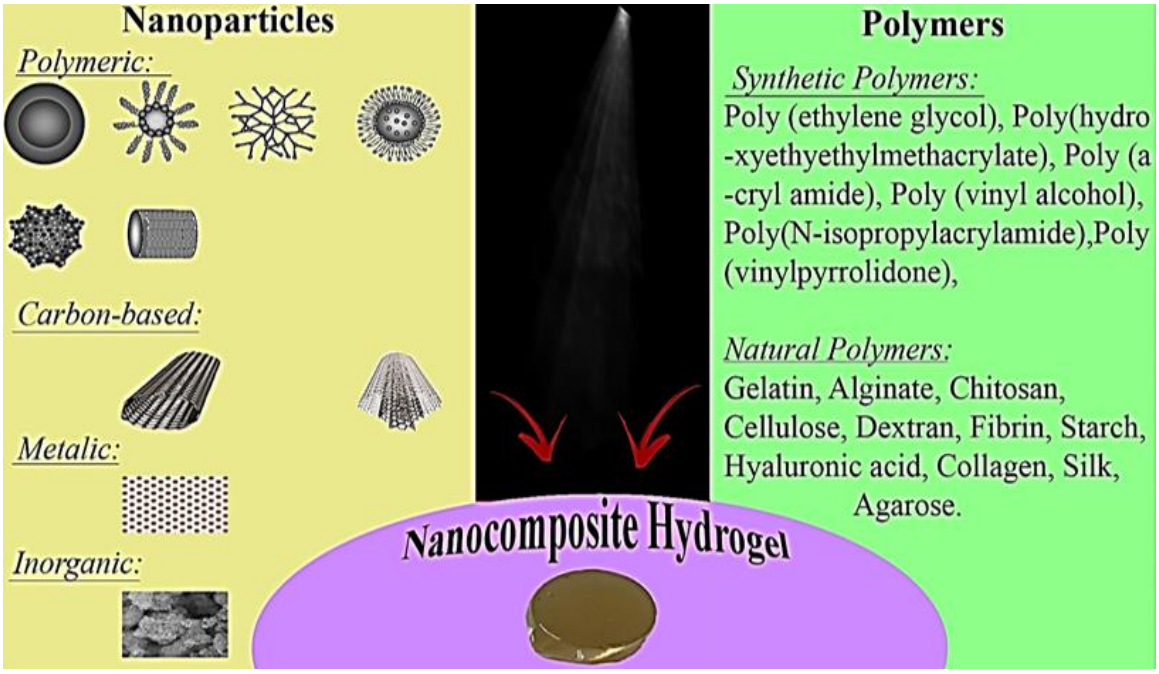

Figure 1.6 A schematic of the formation of the nanocomposites hydrogels with various nanoparticles (adapted from [60]**).**

Due the highly branched and spherical structure [75], polymeric nanoparticles such as dendrimers, hyperbranched polymers, liposomes, polymeric micells, nanogels, and coreshell polymeric particles have come into attention in drug delivery application [76]. Dendritic nanoparticles can easily be crosslinked with hydrogels and the highly branched structure helps to entrap drug, proteins and target release in human body [77]. Hyperbranched poly(amineester) (HPE) nanocomposite hydrogels overcome the drug loading inefficiency by encapsulating hydrophobic drug within the inner cavities of the nanoparticles [78].

Researchers are also inventing new nanocomposite hydrogels using the inorganic nanoparticles present in human body. Combining inorganic ceramic nanoparticles such as HA, synthetic silicate nanoparticles, bioactive glasses, silica, calcium phosphate, glass ceramic, and b-wollastonite [79] with different types of hydrogels provide functional human tissue like scaffolds as well as favorable biological response [80]. Obtaining physiologically stable and highly elastomeric nanocomposite hydrogel was possible by adding HA with poly ethylene glycol (PEG) hydrogel [81]. Incorporating nanosilica with PEG resulted the enhanced mechanical properties and cell adhesion characteristics which can be used as injectable fillers for orthopedic applications [82]. Synthetic silicates nanoparticles, also known as nanoclays, are widely used to reinforce thermoplastic polymers in order to obtain hybrid structures with hierarchical structure, elastomeric properties, ultrastrong and stiff films, super gas-barrier membranes, super oleophobic surfaces, flame-retardant structures, and self-healing characteristic [83], [84]. Not only ceramic nanoparticles are used as reinforcement in polymeric network they are also responsive to biological mechanism, therefore, ceramic nanoparticles have huge potential in the applications of biomedicine [59].

Metal and metal-oxide such as gold (Au), silver (Ag), iron oxide (Fe_3O_4, Fe_2O_3), titania (TiO2), alumina, and zirconia [65] have been in use and showed promising physical characteristics with various hydrogels for imaging agents, drug delivery systems, conductive scaffolds, switchable electronics, actuators, and sensors [65]. Au nanowire incorporated with alginate hydrogel enhanced synchronous and electrical stimulation in neonatal rat cardiomyocytes [85]. External stimuli responsive hydrogels have come in existence due to the adhesion of nano iron and iron oxide which open up the possibility of triggered release of therapeutic agents [86]. Alumina and titania have also used in different applications of

biomedical engineering when infused with hydrogels. Enhanced osteoblast adhesion and proliferation was observed in the alumina and titania based nanocomposite scaffolds [87], [88]. Metal and metal-oxide nanocomposite hydrogels have also showed promises in biosensing, diagnostic, and bioactuation applications [59].

1.5 Research Objective

Maintaining the proper rigidity of the hydrogel for osteogenic tissue engineering without compromising its biodegradability and cell viability has always been a challenge for researchers. Tissues like bone and cardiovascular need rigid and tough scaffolds so that the respective cells can attach and grow within the matrix. It is proven that the organic hydrogels like gelatin methacrylate (GelMA) is biocompatible and biodegradable. But, it inherits the problem of low stiffness as it is a collagen based hydrogel. Increasing the percentage of GelMA and degree of methacrylate may increase the toughness of the gel but it becomes vulnerable place for live cells as GelMA becomes incompatible for cells with the increase of percentage of GelMA and degree of methacrylate. To overcome this challenge, many types of nanoparticles have been infused to the GelMA network in different study yet the stiffness of the hydrogel has not been improved significantly. In this study, clay based nanoparticles which are also readily available in human body in forms of minerals were used to achieve the desire properties of the GelMA. Therefore, the objectives of the thesis are:

1. Design a method to crosslink the nanoparticles with GelMA covalently or physically.
2. Test the feasibility of the developed nanocomposites based on their crosslinkability.

3. Test the mechanical and physical properties of the nanocomposite hydrogel and compare them with pristine GelMA.
4. Test the cell viability of the nanocomposite hydrogel.

To achieve the objectives, two different types of clay based nanoparticles, micro bentonite and nanobentonite, were attempted to crosslink with GelMA network. Micro bentonite and nanobentonite were conjugated with GelMA using ultra violet light (UV) irradiation. Nanosilica was also introduced with the hydrogel to compare its properties with before mentioned nanocomposites. The mechanical properties and microstructures of all nanocomposites were examined by using several material characterization techniques. The biocompatibilities of the nanocomposites were verified by cell encapsulation experiments in 2D environment.

1.6 Chapter Outline

Technique of the development and characterization of a novel biomaterial has been described in this thesis. Chapter 1 discusses briefly the theme of this thesis. An introductory statement about biomedical engineering, hydrogels, nanoparticles etc., and their application in this field was stated. The objectives of the research were discussed. In chapter 2, several techniques of conjugating nanoparticles and their use in different aspect biomedicine were discussed. The process of characterization and testing of feasibility of various nanocomposites were discussed. Chapter 3 discusses the first attempt of conjugating the nanosilica and micro bentonite with GelMA. The mechanical testing, evaluating the microstructure and biocompatibility of the nanocomposites have been verified. In chapter 4, the methodology of the crosslinking process between nanobentonite and GelMA as a novel biomaterial was discussed elaborately. The

physical, mechanical and physiological characterization was described and analyzed. Nanobentonite nanocomposite as bioink is evaluated by printing 3D structure with a 3D printer. Chapter 5 gives a short conclusion and a future perspective of the nanobentonite based nanocomposite research.

Chapter 2: Gelatin Methacrylate Hydrogels

Artificial structure that can mimic natural tissue functions possess significant potential in terms of treating aging, injuries, and diseases [89], [66]. Over the last few decades, new applications of hydrogels have been studied widely all over the world for tissue engineering, stem cell research, and cancer research [61]. Owing to the development of biomolecular engineering, nanotechnology, and polymer chemistry, it is now possible to customize desired properties of hydrogels [63]. This provides the ground for the recent rapid growth of developing hybrid nanocomposite hydrogels as shown in Figure 2.1. Engineers are conjugating different types of inorganic nanoparticles in hydrogels such as CNTs, graphene, GO, HA, nano clay that includes silica, and synthetic silicate nanoparticles, bioactive glasses, calcium phosphate, glass ceramic,

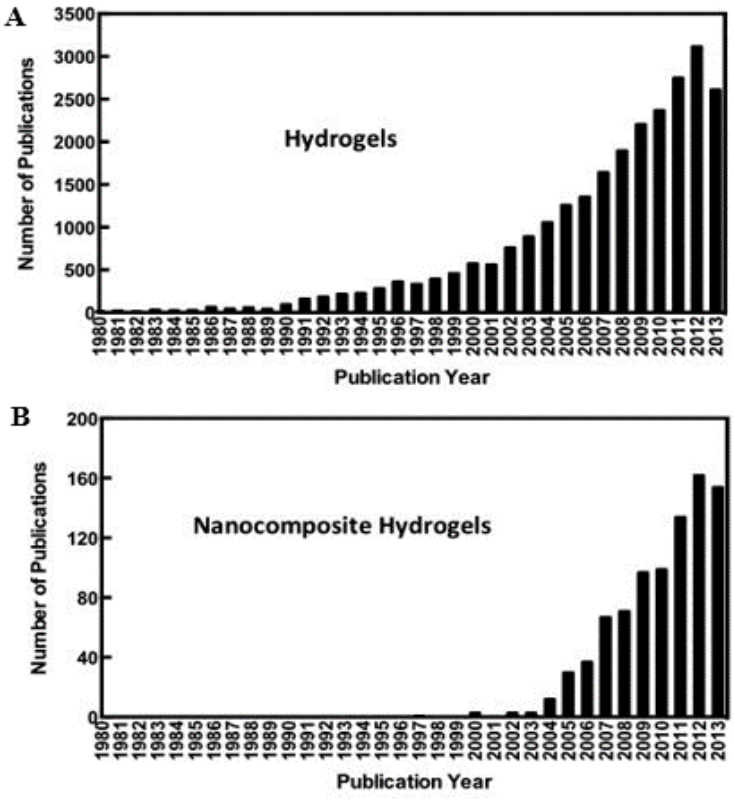

Figure 2.1 (A) Publication related to hydrogel. (B) Publication related to nanocomposite hydrogel (Adapted from [59]**).**

and b-wollastonite for biomedical applications [79], [2], [59].

Gelatin methacrylate (GelMA) is one of most widely used hydrogels in tissue engineering because of its excellent biological characteristics [90]. The microstructural network of GelMA hydrogels resemble native extracellular matrix which allows cells to reproduce and proliferate in numbers. Nanoparticles including carbon nanotubes, graphene oxides, metal oxides, silicates, and many other polymeric nanoparticles can be introduced to GelMA for making hybrid hydrogels [91]. GelMA has been applied to many tissue engineering applications such as bone, cartilage, cardiac, and vascular tissues [2]. GelMA was also used in cell research, cell signaling, drug and gene delivery, and bio sensing [90]. In this chapter, the hybrid GelMA hydrogel with inorganic nanoparticles will be discussed.

2.1 GelMA Hydrogel

Hydrogels can be defined as hydrophilic polymer networks that can absorb water to swell in mass [92]. Synthetic and natural polymers were used to develop various types of hydrogels depending on the cross-linking chemistry and potential biomedical use [93]. However, natural biopolymers work better than synthetic polymers in terms of biocompatibility, low immunoresponse, and chemical structures [90]. Gelatin is a type of natural biopolymers and the hydrolysis product of collagen. It is a main structural protein that can be found in animals connective tissues [94]. Gelatin promotes cell attachment and cell remodeling as it contains arginine-glycine-aspartic acid (RGD) sequences and metalloproteinase (MMP) matrix [94]. Gelatin also shows better solubility and less antigenicity over collagen [95].

Methacrylic anhydride (MA) is used 5% of total molar ratio of gelatin and it does not affect RGD and MMP ensures better cell adhesive property of GelMA [94], [96], [97]. Then, GelMA

undergoes UV irradiation to form a hydrogel [90]. GelMA can be polymerized in room temperature, neutral pH, in aqueous environment and that allows controlling the reaction conveniently [96]. These characteristics are suitable for microfabrication to study cell-biomaterial interactions, and tissue engineering [96], [98].

2.2 GelMA Synthesis

Though there are different protocols exist to prepare GelMA, they are modified from the protocol first proposed by Van Den Bulcke et al. In a phosphate buffer, gelatin reacts with MA at pH=7.4 and 50°C. MA substitution groups and hydroxyl group are reduced to reactive amine and amino acid residues from this reaction [99]. Different amount of MA in gelatin produces GelMA with different physical properties. Higher pH during the reaction intensifies the reactivity between amine and hydroxyl group, resulting in higher degree of substitution [100]. Diluting the reaction mixture (usually five times) with phosphate buffer stops the substitution reaction. Once the reaction is complete, it is dialyzed with membrane filtering tubes for 5-7 days to remove unreacted MA and its byproducts which are potentially cytotoxic. At last, the dialyzed products are kept refrigerated until use [90]. Water soluble photoinitiators under UV are used to crosslink the synthesized GelMA. Two commonly used photoinitiators are 2-hydroxy-1-[4-(2-hydroxyethoxy) phenyl]-2-methyl-1-propanone (Irgacure 2959) [96], [97] and lithium acylphosphinate salt (LAP) [101]. But, LAP is gaining popularity over Irgacure 2595 because of high solubility and high molar extinction coefficient at 365nm [101]. A general process to synthesis GelMA hydrogels is shown as a flow chart (Figure 2.2).

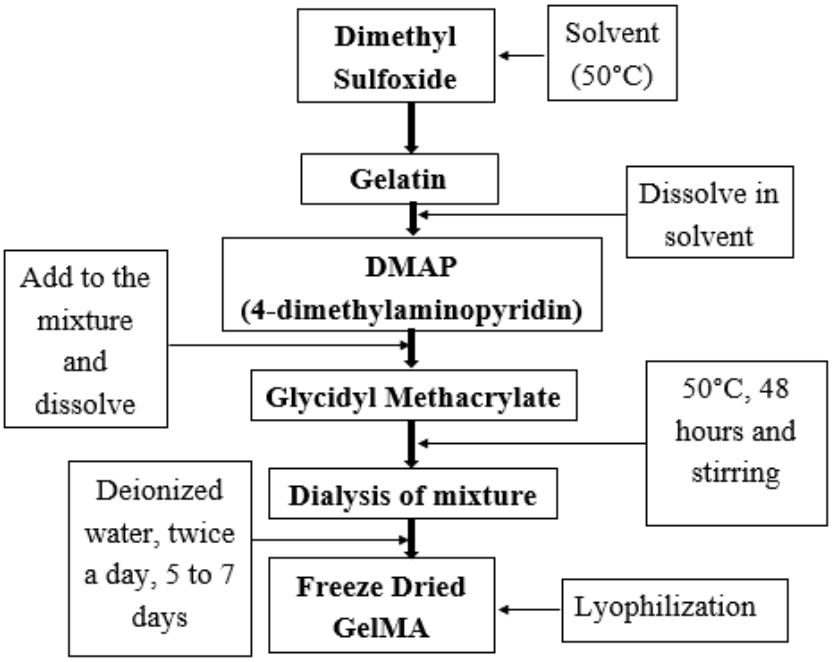

Figure 2.2 General process of GelMA hydrogel synthesis.

2.3 Physical Properties of GelMA

The parameters that are responsible for tuning the physical properties of GelMA are the degree of substitution, macromer concentration, photoinitiator concentration, and UV exposure time [99]. GelMA offers the flexible tuning of its properties if manipulation of its synthesis process is done while crosslinking [90]. Several studies reported that the elastic modulus of GelMA can be changed by adding varying degree of methacrylate substitution.

Koshy et al. claimed that cryogenic treatment (i.e. freeze drying) could produce porous scaffolds of GelMA with controlled pore sizes and porosity [102]. And Vlierberghe et al. showed that average pore sizes in GelMA scaffolds were inversely related to the cooling rate and they prepared different pore sizes of GelMA using the gradient cooling rate strategy [103]. The varying degree of methacrylate substitutions also change the pore sizes in GelMA scaffolds [90], [104], [105].

Chen et al. also proposed that the elastic modulus of GelMA hydrogel is directly proportional to the degree of methacrylate substitution. Elastic modulus is also directly proportional to the mass/volume fraction of the GelMA solution [96]. They also showed that the swelling ratio of the hydrogel is inversely proportional to the methacrylate substitution and the GelMA mass/volume fraction. Cell proliferation rate was decreased with the increase of GelMA mass/volume fraction The advantage of GelMA hydrogel is that it can be utilized in cell culturing in both 2D and 3D experiments., It is compatible biologically and mechanically with the native extra cellular matrix [106]. For example, the incorporation of cells in prepolymer GelMA solution and crosslinked with UV light exposure to form cell-laden 3D hydrogel scaffolds. The advantage of 3D hydrogel scaffolds over 2D cell culture is that photocrosslinked 3D cell culture is 80% viable to native ECM [97]. Some direct relationships such as pore size, elastic modulus, swelling ratio, and cell proliferation can be tabulated from this paragraph (Table 2.1).

Table 2.1 Relationship between different physical properties of GelMA.

Parameter	Relation
Pore Size	Inversely related to the cooling rate. [106],[103]
	The change of pore size depends on degree of methacrylate substitutes. [90], [105], [104]
Elastic Modulus	Directly proportional to the degree of methacrylate substitutes. [105]
	Directly proportional to the mass/volume ratio of the GelMA solution. [96]
Swelling Ratio	Inversely proportional to the methacrylate substitutes. [96]
Cell proliferation	Decreases with the increase of GelMA mass fraction in hydrogel. [96]
3D cell culture	80% viable to the native cell culture. [97]

2.4 GelMA with Nanoparticles

Since the GelMA hydrogels have been developed, researchers have examined them thoroughly in the perspective of adaptability with the body and found many suitable physical and biochemical properties for tissue engineering, biosensing, drug delivery [39]. In these sections, interactions between GelMA hydrogel and different nanoparticles, and their properties and the change of characteristics of GelMA after adding different types of nanomaterials are discussed.

2.4.1 GelMA with Carbon Nanoparticles

Since the discovery of CNTs, researchers have been harnessing its potentials such as high aspect ratio, stiffness, light weight, superior electrical properties, chemical and thermal stability to use it in biomedical and biological fields. Ma et al., claimed that modification of CNTs surfaces with amines (NH2), hydroxyls (OH), and carboxyls (COOH) facilitated the CNTs disperse in hydrophilic polymer to overcome the drawback. Gaharwar et al. examined other techniques such as singe-stranded DNA (ssDNA), proteins, and surfactants to increase the solubility of the CNTs and they reported that significant improvement was observed for the dispersion rate. One way to shield the CNTs is to hybridize with amyloid fibrils to produce fibrous hydrogel [72]. They observed that adding amyloid fibrils with CNTs decreased the gelling concentration and increased the interactions between polymer and nanotubes. Many proteins create amyloid fibrils and CNTs-GelMA shielded with proteins are envisaged to generate hydrogels for tissue engineering, drug delivery, and biosensing [72].

Some tissue engineering applications requires stiffer hydrogel which cannot be obtained generally from GelMA hydrogel (up to 30 kPa in elastic modulus) [90]. 15% or more concentration of GelMA can produce high strength polymer but that affects the degradability, porosity, cell

proliferation and growth [90]. Hybrid hydrogel, nanoparticles incorporated GelMA is an alternative to enhance mechanical properties of GelMA hydrogel for suitable scaffolds for cell growth [107], [108]. Shin et al. reported that CNTs in GelMA increased the stiffness without affecting the porosity and 3D cell growth. Shin et al. also reported that incorporation of CNTs of 0.5 mg/mL in GelMA showed a maximum elastic modulus of 31±2.4 kPa for a 5 W/V % of GelMA, which is much better than the observed virgin 5 W/V% GelMA hydrogel (10±0.5 kPa). Furthermore, bioprintable ink for 2D and 3D tissue engineering has also emerged from CNTs and bio-surfactants such as DNA, HA, and GelMA were used to make it stable in aqueous solution and biological fluids, cytocompatible, flexible, foldable, and blendable for 2D and 3Delectronic circuits [109]. The scope and promises of the CNTs-GelMA hydrogels are summarized in Table 2.2.

Table 2.2 Different aspects of CNTs-GelMA hybrid hydrogels.

Hydrogel	Additional Component	Remarks
CNTs-GelMA	NH_2, OH, COOH	Accelerate dispersion of CNTs in hydrophilic polymer. [110]
	ssDNA, proteins, and surfactants	Improvement in dispersion rate of CNTs in hydrophilic polymer. [59]
CNTs-GelMA	COOH	Nanofibrous mesh like network viable with cardiac tissue. [108]
GelMA	0.5% CNTs	Tensile modulus is creased by three folds. [108]
GelMA	CNTs	Superior electric conductivity used in nerve, muscle, and cardiac tissue. [59]
GelMA	CNTs	Beating rate of cardiomyocytes by three folds. [107]
CNTs-GelMA	Amyloid fibril	Increase the solubility of CNTs. [72]
GelMA	0.5 mg/mL CNTs in GelMA	Maximum elastic modulus of 31±2.4 kPa. [107]
GelMA	CNTs	85% to 100% cell viability. [107]

2.4.2 GelMA with Graphene Nanoparticles

Graphene is a carbon-based nanomaterial that is used in hydrogel as the sheet of GO to enhance the solubility within the hydrophilic polymer [59]. One study suggested that less than 1% surface atoms was enough to increase one order of magnitude of mechanical properties if GO conjugates with polymer chains covalently [111]. Recently, Liu et al. devised a technique to covalently conjugate GO sheets to GelMA hydrogels [74]. The methodology included radiation induced peroxidation of GO to obtain GPO. Then, covalent crosslinking took place between GPO and GelMA hydrogels [74]. 900% increase in tensile strength and 500% tensile elongation were reported due to the covalently addition of GPO (3 mg/L) with GelMA hydrogel compared with GO-GelMA hydrogels. Tissues that are subjected to constant mechanical stress and electrical stimulation could use these covalent crosslinking approach to form elastomeric scaffolds [59]. Viability between the mammalian cells and these hybrid hydrogels are rarely studied, therefore, further investigation is required although GPO enhanced the mechanical properties of hydrogels. GO-GelMA hybrid hydrogels are successful to enhance many mechanical and physical properties of hydrogels and they are listed in (Table 2.3).

Table 2.3 Different aspects of Graphene-GelMA hydrogel.

Hydrogel	Additional component	Remarks
GelMA	GO	One order of magnitude of mechanical properties increased by 1% surface atoms while conjugated covalent. [111]
GelMA	3 mg/mL of GPO	900% increase in tensile strength and 500% tensile elongation. [74]
GelMA	MeGO	Resistance to fracture and 11 time better ultimate stress. [112]
GelMA	GO	60% higher fibroblast proliferation than virgin GelMA. [112]
GelMA	fGO	Increase of myocardial capillary density and decrease of scar extension. [113]
GelMA	GO	Elastic modulus can be increased by 36% and electrical conductivity by two folds. [114]

2.4.3 Inorganic Nanoparticles

Inspired by the knowledge that human body holds many inorganic minerals [80] such as calcium, phosphate, silica etc., researchers are devising biohybrid nanocomposite hydrogels to develop and maintain the workability of different parts of the body [59]. e.g. calcium and phosphate deposit in bone and silicon takes part in skeleton development as wells as differentiates human stem cells and synthesis collagen type 1 [59]. In addition, minerals play a crucial role in the normal homeostasis and turnover of human tissues which are favorable biological cues for the ceramic minerals in hydrogels [80] as well as these inorganic nanoparticles reinforce the hydrogel due to their high mechanical strength [115], [2].

Nanosilicates have been used recently [116] to conjugate with GelMA hydrogel. 2D nanosilicates increased pore size from 0.2-0.9μm to 0.3-1.5 μm, and elastic modulus by four times when compared with pristine GelMA. GelMA-nanosilicates hydrogel promoted preosteoblast NIH MC3T3 cells' osteogenesis even without the osteoinductive growth factor in the media. Another study showed that the polymeric hydrogel got elongated with the incorporation silicates while forming crosslinked network [117]. GelMA crosslinked with nanosilicates could support differentiation of osteogenic stem cells without the presence of any pharmaceutical growth factor [118]. Among other things, GelMA with nanosilicates showed the ability to regenerate bone [116] and stop internal hemorrhage by enhancing hemostasis [119]. The promises and prospects of this section are tabulated in (Table 2.4).

Table 2.4 Different aspects of nanosilicates-GelMA hydrogel.

Hydrogel	Additional Material	Remarks
GelMA	Nanosilicates	Increase the pore size from 0.2-0.9 μm to 0.3-1.5 μm. [116]
GelMA	Nanosilicates	Elastic modulus increased by four times. [116]
GelMA	Nanosilicates	Injectable tissue repairing matrices, bioactive filler, and therapeutic agents. [117], [84]

2.4.4 Metal Oxide

Schexnailder and Schmidt reported that metal and metal oxide such as gold (Au), silver (Ag), iron oxide (Fe_3O_4, Fe_2O_3), titania (TiO_2), alumina, and zirconia have been used to fabricate nanocomposite hydrogels [65]. Some researchers showed that Gold [120], [121], minerals [122], [16], and titanium [123] nanoparticles with GelMA hydrogels have used to promote osteogenesis, protect cells while culturing with GelMA hydrogels, promote osteoconductivity and induce osteogenic differentiation, and enhance osseointegration respectively.

It is seen that the bonding capacity between the hydrogels and the metal/metal-oxide nanoparticles are relatively weak [59]. However, Balazs et al. and Caruso et al. enhanced the interaction between polymer and nanoparticles by functionalizing the surface of nanoparticles [124], [125]. Functionalized surface of nanoparticles gives the opportunity to enhance the physical, chemical, and biological properties of hybrid hydrogels. Heo et al. incorporated gold nanoparticles (GNP) in GelMA hydrogel for bone tissue engineering and this GelMA hybrid enhanced cell proliferation and differentiation [121]. As metals are electrically conductive, researchers [85] incorporated gold nanowire within alginate hydrogels to increase the electrical conductivity. Gold nanowire grafted in alginate hydrogels promoted electric signal to align functional tissues, contracted synchronously neonatal rat cardiomyocytes, and increased cardiac beats when compared with alginate hydrogels [85].

García-Astrain et al., developed hybrid gelatin based hydrogels infused silver nanoparticles. These hybrid hydrogels based on gelatin and chondroitin sulphate crosslinked with silver nanoparticles showed better storage modulus, lower swelling ratio and higher cell compatibility relative to the nanoparticle free hydrogel which made this hybrid hydrogel a potential candidate for drug delivery system [126]. To obtain stimuli-responsive hydrogel, magnetic nanoparticles

can be conjugated with biocompatible and thermoresponsive hydroxypropyl cellulose [86]. This heat generating hybrid hydrogel can be used to release therapeutic agents or cells from the nanocomposite hydrogels. Price et al., and Webster et al. created alumina and titania based hydrogel for enhanced osteoblast adhesion and cell proliferation [87], [88]. But, researchers rarely study these hybrid nanoparticles as metal/metal oxides attribute less interaction within the polymer.

However, functionalized surface of titania was introduced to overcome the problem as a recent study showed that titania with amine groups encouraged covalent interaction between nanoparticles and carboxymethylcellulose [127]. It can be used to encapsulate cells for tissue engineering. GelMA hydrogel was used to modify the titanium surface for protein adsorbsion [129]. GelMA coated titanium surface showed greater bioactivity with higher affinity to proteins over uncoated titanium surface [128]. Si et al., showed that the GelMA hydrogels with in situ generated TiO_2 had antibacterial activities against *E. coli* and *S. aureus* without cytotoxicity [130]. The main idea of this section is summarized in (Table 2.5).

Table 2.5 Different aspects of metal nanoparticles-GelMA hydrogel.

Hydrogel	Additional Component	Remarks
GelMA	GNP	Bone tissue engineering, cell proliferation, and differentiation. [128]
GelMA	Ti	Enhance osseointegration in bone tissue. [128]
GelMA	HA	Increase adhesion between cells. [81]
GelMA-HA	PEG	Highly elastomeric. [81]
GelMA	Gold nanowires	Increase electric conductivity, and cardiac beat rate. [85]

2.5 Summary

Nanocomposite biohybrid hydrogels are having great potentials for biomedical and pharmaceutical aspects that includes drug delivery, stem cell engineering, regenerative medicine, actuators, sensors, and biomedical devices. Hybrid hydrogels show higher mechanical, chemical, biological, electrical, and physical properties. But, some gaps are still there which needed to be resolved. Nanoclay based hybrid hydrogel showed great potential in the applications of antimicrobial films, injectable drug delivery matrix, and cell adhesion surfaces yet a few studies have been conducted in this field [131]. Overall, metal oxide, ceramic nanoparticles along with carbon nanotubes show favorable biological response such as electrical conductivity, scaffolding, resembling, and cell proliferation in various biomedical applications. Therefore, investigation on the different biological properties are required to design next generation hydrogel. The future technologies will be devised such a way that hydrogel can replicate native tissues without any cytotoxic issues. Moreover, focus will be given on the understanding of interaction between hydrogels and nanocomposite materials. More preciously, the ultimate goal is to create a multifunctional hydrogel which can be used numerous biomedical application.

Chapter 3: GelMA with Micro Bentonite and Nanosilica

In chapter 2, an overview of the nanocomposite hydrogels using GelMA and inorganic, ceramic, metal oxide, and carbon-based nanoparticles in the last decade was presented. These acquired knowledge helped us to initiate the processing and characterization of hybrid GelMA using clay based material. As clay has been used widely in modern medicine for a long time yet its use in biomedical engineering is still infancy [132], [91]. The purpose of the study was to design a GelMA based nanocomposite that could exhibit better rigidity and toughness in GelMA as this was one of the main criteria of bone tissue engineering using hydrogel graft.

3.1 Characterization of Particles

3.1.1 Micro Bentonite

Clay bentonite was provided from the Geotechnical Lab, University of British Columbia, Okanagan Campus. To know the average particle size of the bentonite, it was scanned under (SEM). The average particle size found were more than 1.2 to 2.1 µm which is shown in figure 3.1. Geotechnical lab confirmed the liquid limits and plastic limits were 127.3% and 72.21%

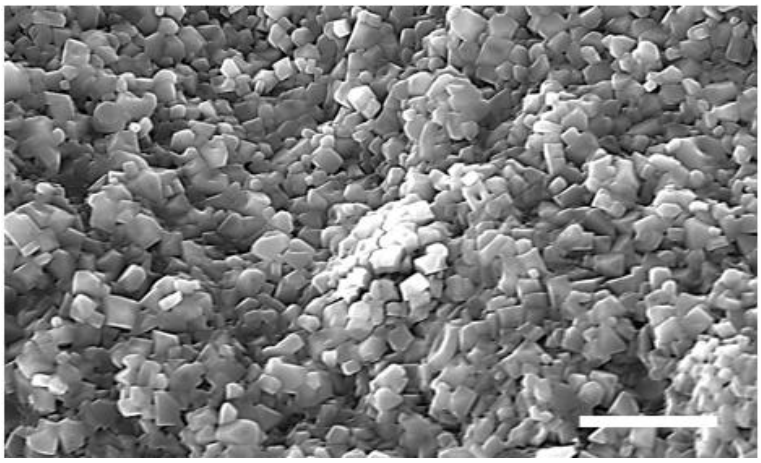

Figure 3.1 Particle size analysis for micro Bentonite under SEM (Tescan Mira3 XMU Field Emission Scanning Electron Microscope), bar represents 10 µm.

respectively. No swelling was observed after soaking 10g of soil in distilled water for 24 hours. The bentonite clay was comprised of minerals like montmorillonite, albite, quartz, christobalite, and anorthite. Details of XRD and X-ray Fluorescence (XRF) analysis of bentonite clay is presented in table 3.1 and table 3.2 respectively [58].

Table 3.1 Mineralogical composition of bentonite in micro scale.

	Montmorillonite	Albite	Quartz	Anorthite	Illite
Bentonite	76.3	12.9	10.4	0	0

Table 3.2 Chemical composition of bentonite and bentonite nanoparticles.

	(Na^{+})	(K^{+})	(Ca^{2+})	(Mg^{2+})	(Al^{+})	(Si^{2+})	(O^{2-})	(Cl^{-})
Bentonite	1.58	1.52	0.92	1.49	11.4	33.5	47.2	0.63

3.1.2 Nanosilica

Nanosilica was purchased from MK nano, MK Impex Corp., Canada. The physical properties claimed by the company was that the average size of the nano particles was 15 nm, they were hydrophobic, and they were 99.5% pure. The particles were confirmed under the SEM which were in nano scale (figure 3.2). The elemental analysis from the energy dispersive spectroscopy (EDS) confirmed the that the nanosilica consisted of silicon (Si), and (oxygen) O, and trace amount of sodium (Na), sulfur (S), and aluminum (Al) (figure 3.6A).

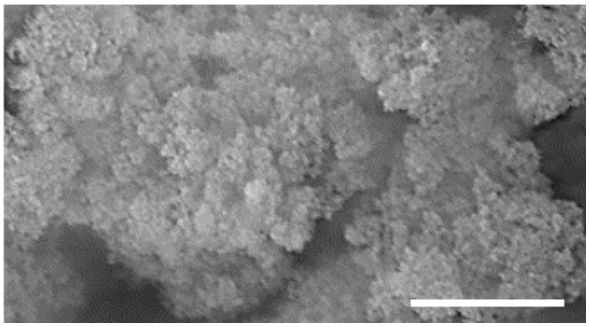

Figure 3.2 SEM image of nanosilica. Scale bar = 2 µm.

3.2 Crosslinking of GelMA Composites

3.2.1 GelMA with Micro Bentonite

At first, 5% pristine GelMA was made to test as control. Methacrylate group was added to the dissolved gelatin and dialysis process was initiated to purify the solution for seven days. Then, through lyophilization process, addition water was removed from the pre-polymer solution. Later, freeze-dryed matrix was dissolved in phosphate buffer solution, (PBS) and 0.5% (w/v) Irgacure 2959 was added to crosslink the solution under UV radiation to obtain GelMA polymer.

In an attempt to crosslink the micro bentonite with the GelMA network, a solution of micro bentonite and photoinitiator was made with PBS. An ultra sonication probe (Vir Sonic 100, Vir Tis) was used for 15 minutes to disperse the micro bentonite and photoinitiator into the PBS. Subsequently, this solution was added to the pre-polymer GelMA solutinion and put it in a vortex machine (VWR Analog Vortex Mixer) for 30 minutes to get a mixture of GelMA prepolymer and solution of micro bentonite and photoinitiator. Later, the solution was placed under the UV irradiation to crosslink the polymer. Figure 3.3 indicates the gel formation of pristine GelMA and GelA with micro bentonite. The integration of the micro bentonite with the GelMA polymer was needed to be checked. So, the samples of freeze-dried GelMA and GelMA with micro bentonite were placed under SEM to get the micro structure of the samples (figure 3.4). After adding the

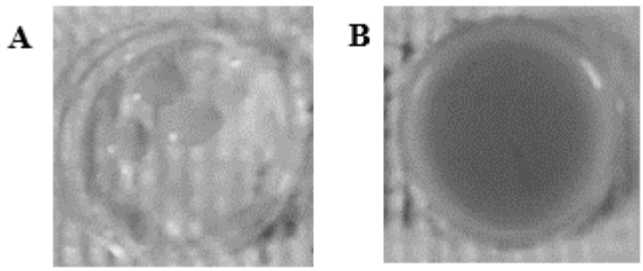

Figure 3.3 Represantative crosslinked samples around 1 cm in diameter of (A) pristine GelMA and (B) GelMA with micro bentonite.

micro bentonite, the pore size of the hydrogels did not change and the clay particles seemed to be agglomerated. Agglomerated particles were the evidence that the particles were not well bonded with the hydrogel polymer and also this affected the dispersion rate of the particles into the polymer matrix. In the figure 3.3, 5% w/v pristine GelMA was scanned and average pour size was found to be between 4.75-10.5 µm. After adding the micro bentonite, the pore of the hydrogel was not visible and the agglomeration of particles occurred. At the higher concentration of micro bentonite, the particles were seen lying on the GelMA without interacting with the chain.

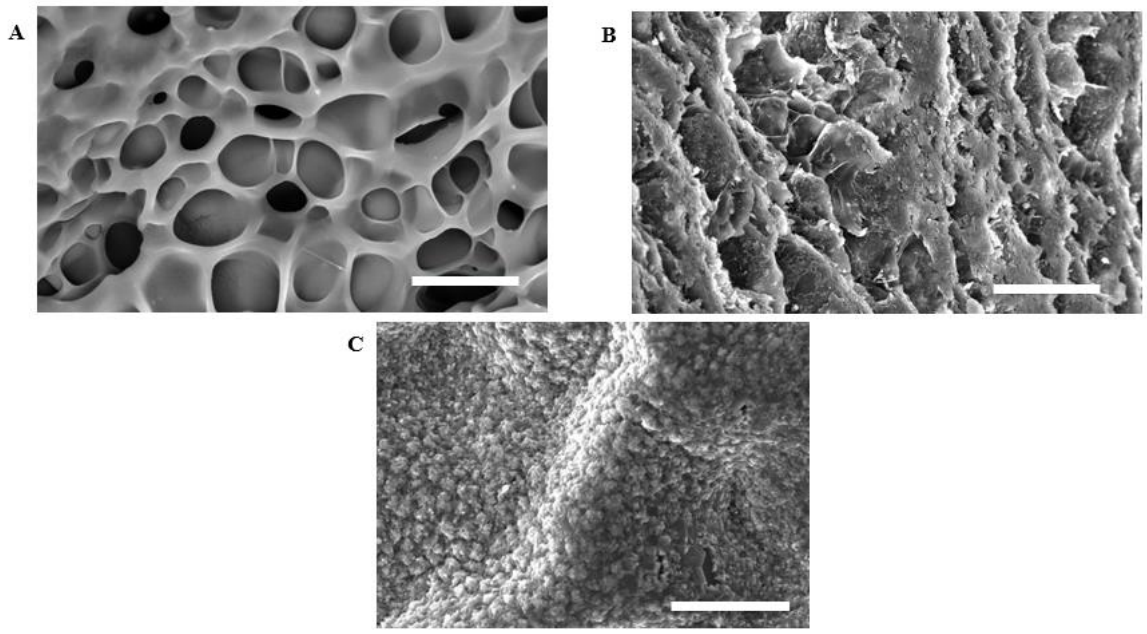

Figure 3.4 Micro structure of GelMA and hybrid GelMA after adding micro bentonite. (A) 5% GelMA. Scale bar = 20 µm. (B) 5% GelMA with 0.2% micro bentonite. Scale bar = 50 µm (C) 5% GelMA with 0.5% micro bentonite. Scale bar = 50 µm.

3.2.2 GelMA with Nanosilica

Similar to the micro bentonite experiments, at first, 5% pristine GelMA was made to test as control. Methacrylate group was added to the dissolved gelatin and dialysis process was initiated to purify the solution for seven days. Then, through lyophilization process, addition water was

removed the pre-polymer solution. Later, freeze-dryed matrix was dissolved in PBS and 0.5% (w/v) Irgacure 2959 was added to crosslink the solution under UV radiation to obtain GelMA polymer.

In an attempt to crosslink the nanosilica with the GelMA network, a solution of nanosilica and photoinitiator was made with PBS. An ultra sonication probe (Vir Sonic 100, Vir Tis) was used for 15 minutes to disperse the nanosilica and photoinitiator into the PBS. Subsequently, this solution was added to the pre-polymer GelMA solutinion and put it in a vortex machine (VWR Analog Vortex Mixer) for 30 minutes to get a mixture of GelMA prepolymer and solution of micro bentonite and photoinitiator. Later, the solution was placed under the UV irradiation (UVL-28 ELSeries UV Lamp, 365 nm) to crosslink the polymer. Figure 3.5 indicated the gel formation of pristine GelMA and GelA with nanosilica.

The integration of the nanosilica with the GelMA polymer was needed to be checked. Elements of GelMA was checked under EDS and the elements found were C, O, N, Cl, K, and Na. After infusing the nanosilica with GelMA, elemental analysis was also performed and the elements found in there both matched with nanosilica and GelMA (figure 3.6 B, C). To be

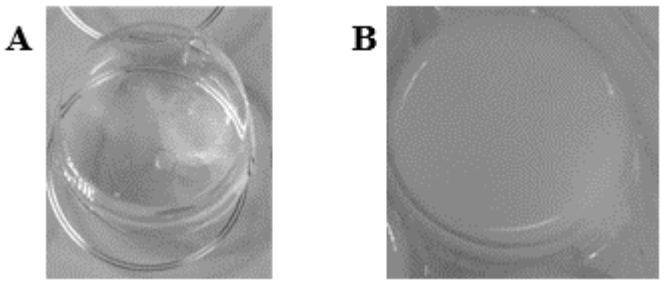

Figure 3.5 Represantative crosslinked samples around 1 cm in diameter of (A) pristine GelMA and (B) GelMA with nanosilica.

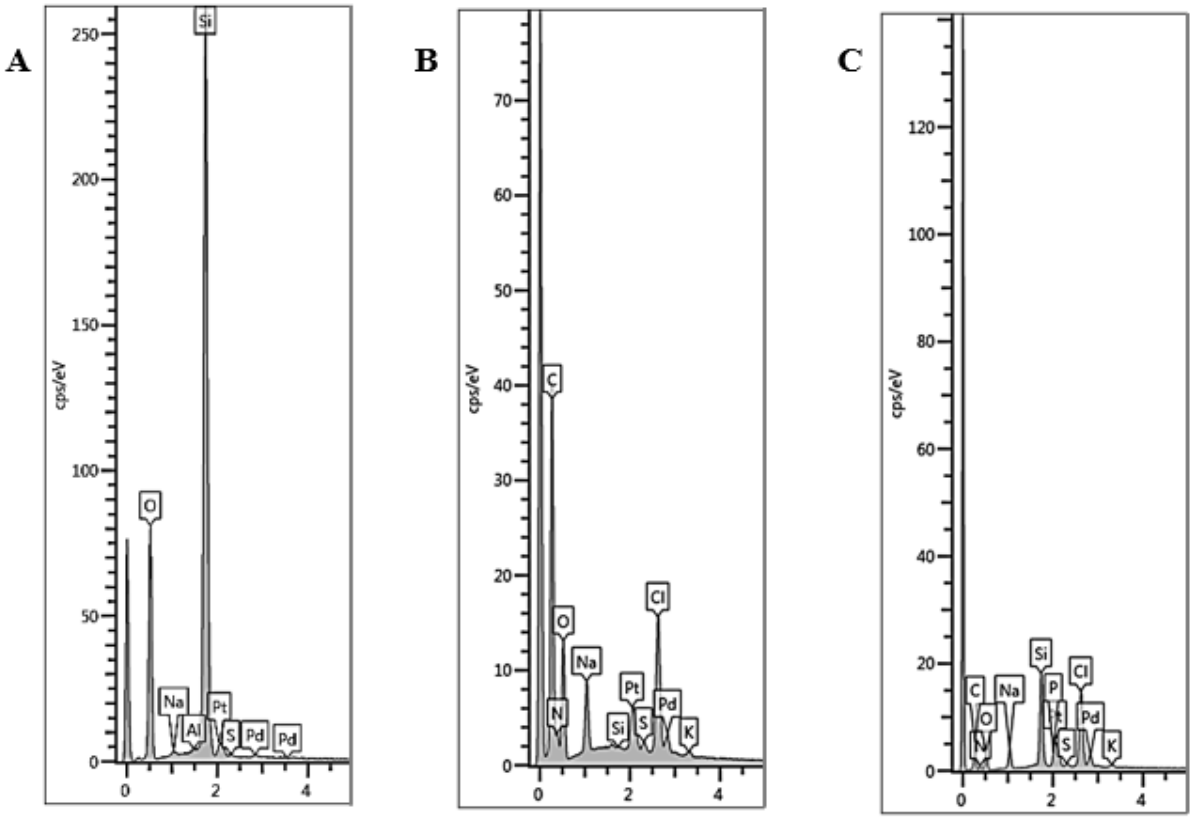

Figure 3.6 EDS analysis of GelMA and hybrid GelMA after adding nanosilica. (A) EDS of nanosilica. (B) EDS of GelMA hydrogel. (C) EDS of GelMA hydrogel with nanosilica.

more certain, the samples of freeze-dried GelMA and GelMA with nanosilica were placed under SEM to get the micro structure of the samples (figure 3.7). After adding the nanosilica, the pore size of the hydrogels increased and very little agglomeration among particles occured.

Little agglomerated particles are the evidence that the particles are well bonded with the hydrogel polymer at this point and most of the nano particles dispersed with hydrogels properly. In the figure 3.7, 5% w/v pristine GelMA was scanned and average pore size was found to be between 4.75-10.5 µm. After adding the 0.2% w/v nanosilica, the pore size of the GelMA increased to 17.5-24.1 µm. 0.5% w/v addition of nanosilica increased the pore size to 23.5-36.8 µm. And, 1% w/v of nanosilica increased the pore size ranging between 31.5-53.25

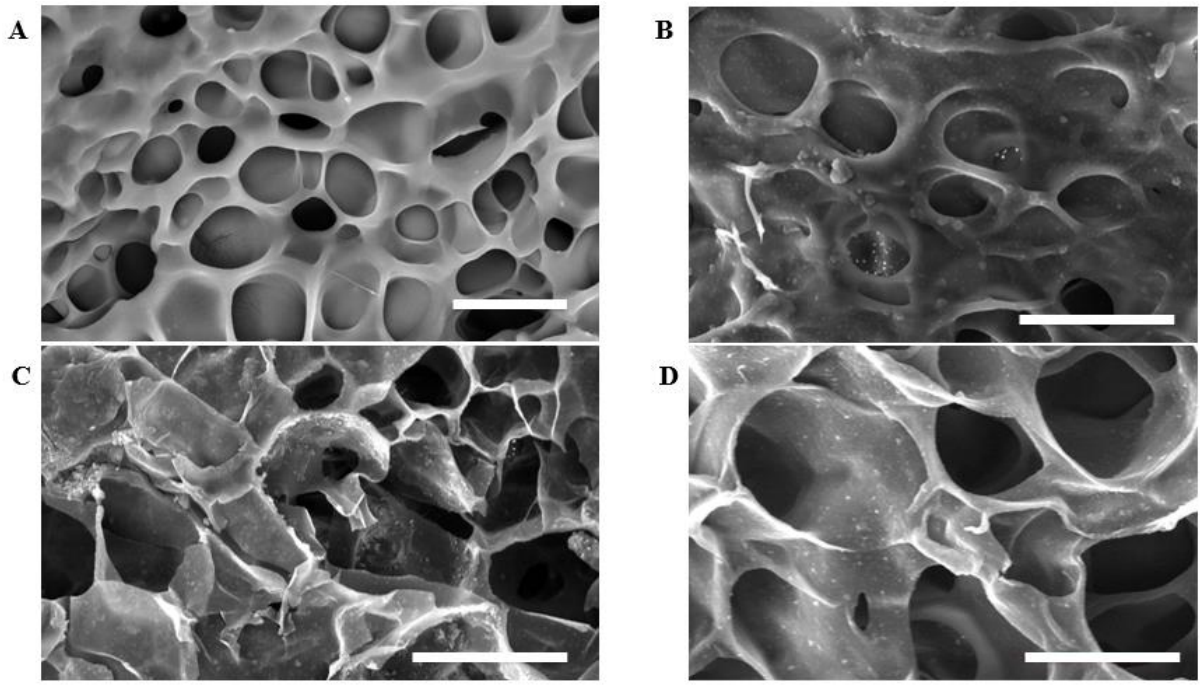

Figure 3.7 Micro structure of GelMA and hybrid GelMA after adding nanosilica. (A) 5% GelMA, scale bar = 20 µm. (B) 5% GelMA with 0.2% nanosilica, scale bar = 50 µm. (C) 5% GelMA with 0.5% nano silica, scale bar = 20 µm. (D) 5% GelMA with 1% nanosilica, scale bar = 20 µm.

µm. A 7 fold increase of pore size occurred to the prisine GelMA after adding 1% nanosilica. Increase in the pore size indicates that nanosilica is interacting with the GelMA polymer very well. Large pore size also provides the opprtunity for cells to grow healthy and proliferate well in the pores.

To further study the interaction between the nanosilica and GelMA hydrogel, Fourier transform infrared spectra (FT-IR) was used to observe the transmittance with respect to the wavenumber of the materials (figure 3.8). Nanosilica gave the peak of Si-O-Si between 1000 and 1200. The amides peaks of GelMA were observed at 1500 and 1600. Hybrid GelMA conjugated with nanosilica provided both Si-O-Si and amides indicating that nanosilica and polymer chains of GelMA were interacting very well in the matrix.

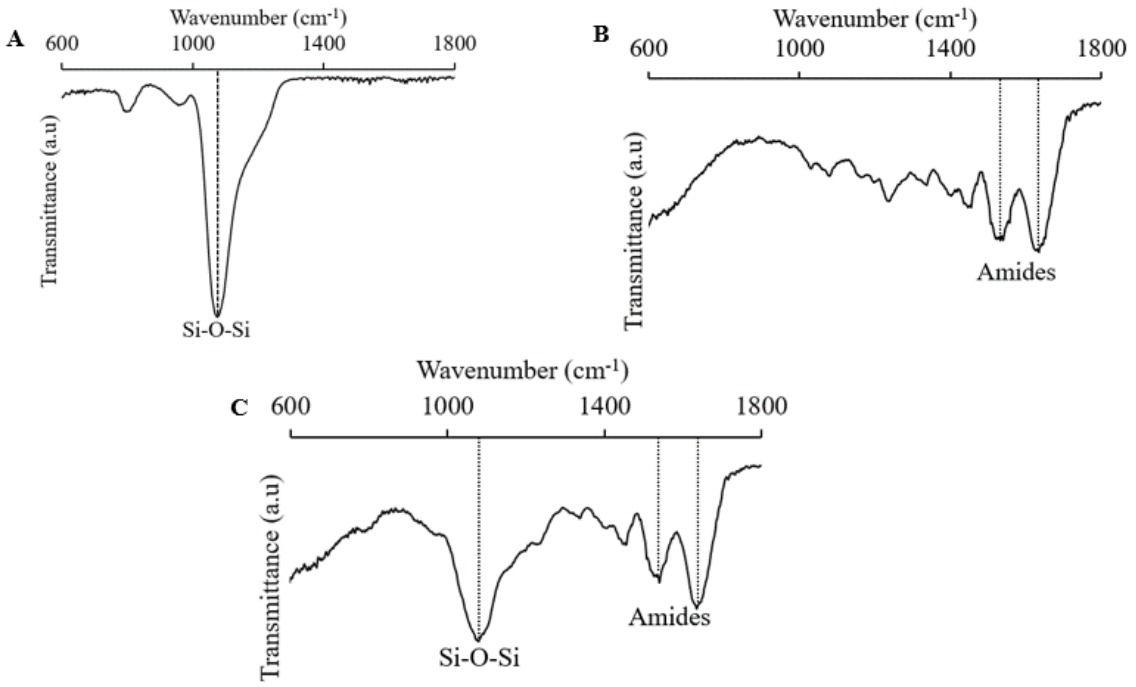

Figure 3.8 FT-IR spectra of hybrid hydrogel. (A) Silica nanoparticles with Si-O-Si peak. (B) Pristine GelMA with amides peaks. (C) Hybrid nanosilica GelMA with both Si-O-Si and amides peaks.

3.3 Mechanical Characterization of GelMA Composites

3.3.1 GelMA with Micro Bentonite

As the main objective of this study is to increase the toughness of the GelMA, therefore, the elastic modulus of GelMA was measured after inserting the micro bentonite. So, samples of pristine 5% w/v GelMA and 0.2% and 0.5% micro bentnite with GelMA were synthasized. Five cylindrical specimens (6 mm in diameter) from each type of GelMA and the mentioned concentration of micro bentonite with GelMA hydrogels were cut from the petri dish using a punch. The elastic modulus of each sample was tested by a dynamic mechanical analyzer (DMA, Q800, TA Instruments, New Castle, DE, USA). The elastic modulus was calculated from the slope of the linear region between strains from 5% to 15% as shown in figure 3.9. One-way analysis of variance (ANOVA analysis)

function in Microsoft Excel 2016 (Microsoft Corp., USA) was used to statistically analyze the data obtained from the experiments. Results are shown in the form of mean ± standard deviation. The sample size for the whole study was taken between 3 to 5 due to the time-consuming nature to fabricate the samples.

The elastic modulus of the 5% w/v GelMA was 6.25 ± 0.65 kPa which was consistent to the previous studies [90]. Adding of 0.2% w/v micro bentonite to the GelMA increased the elastic modulus 6.9 ± 0.57 kPa which was insignificant compared to the strength of the pristine GelMA. After increasing the concentration of micro bentonite to 0.5% w/v, the elastic modulus of the hybrid GelMA reduced to 5.2 ± 0.24 KPa. This indicated that micro bentonite did not help GelMA to increase its toughness rather it did reduce the stiffness. As, the particles did not react with the polymeric chains, rather they were responsible for blocking the UV irradiation for the GelMA network to get crosslinked. The size of the particles may also be responsible for being inert inside the polymeric chains as charged tails in the micro particles are close to null.

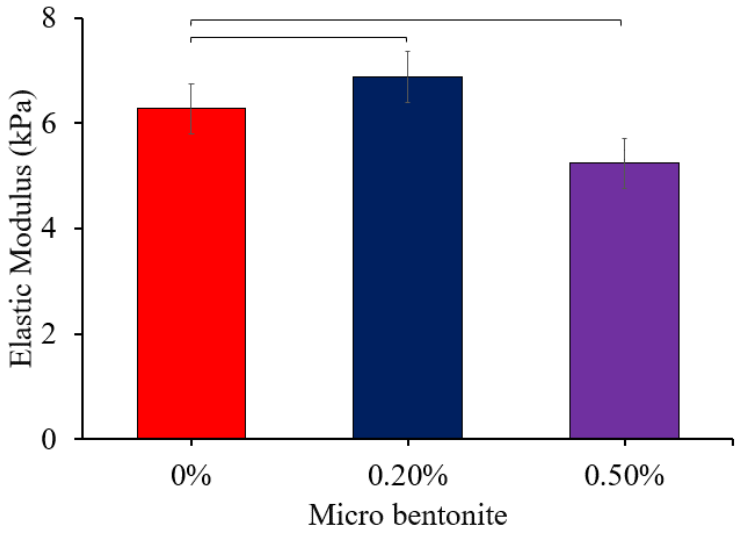

Figure 3.9 Characterization of the mechanical properties of micro bentonite hybrid GelMA: Determining the elastic modulus of 5% GelMA and various concentration of micro bentonite with GelMA (n=5).

3.3.2 GelMA with Nanosilica

At first, the elastic strength was measured for both GelMA and hybrid GelMA with nanosilica. So, samples of pristine 5% w/v GelMA and 0.2%, 0.5%, and 1% nanosilica with GelMA were synthasized. Five cylindrical specimens (6 mm in diameter) from each type of GelMA and the mentioned concentration of nanosilica with GelMA hydrogels were cut from the petri dish using a punch. The elastic modulus of each sample was tested by a dynamic mechanical analyzer (DMA, Q800, TA Instruments, New Castle, DE, USA). The elastic modulus was calculated from the slope of the linear region between strains from 5% to 15% as shown in figure 3.10. One-way analysis of variance (ANOVA analysis) function in Microsoft Excel 2013 (Microsoft Corp., USA) was used to statistically analyze the data obtained from the experiments. Results are shown in the form of mean ± standard deviation.

The elastic modulus of the 5% w/v GelMA was 6.25 ± 0.65 kPa which was consistent to the previous studies [90]. Adding of 0.2% w/v nanosilica to the GelMA increased the elastic

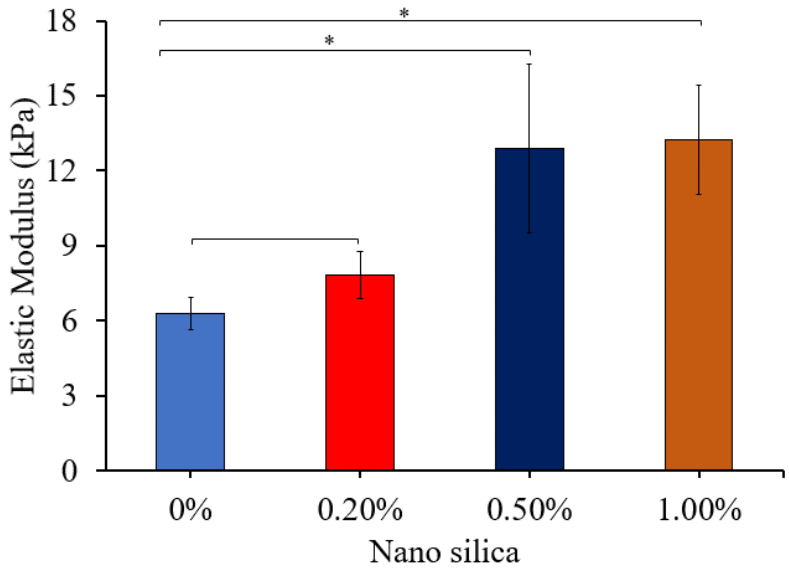

Figure 3.10 Characterization of the mechanical properties of nanosilica hybrid GelMA: Determining the elastic modulus of 5% GelMA and various concentration of nanosilica with GelMA (*p<0.05, n=5).

modulus 7.84 ± 0.94 kPa which was insignificant compared to the strength of the pristine GelMA. After increasing the concentration of nanosilica to 0.5% w/v, the elstic modulus of the hybrid GelMA raised to 13 ± 3.38 kPa. 1% of nanosilica increased the elastic modulus to 13.25 ± 2.18 kPa which was noteworthy comparing the rise of the concentration of the nano particles.

The two folds increase of the stiffness of the GelMA due the 0.5% and 1.0% nanosilica were the evidence that nano particles were interacting well with the polymeric chains of the hydrogel. Although, 13 kPa was not enough to use in bone tissue engineering rather it can be used other soft tissue engineering. It was also evident that 0.5% is the optimum concentration of nanosilica which can be used in GelMA to tailor its toughness.

Mass swelling ratio of the samples were also measured (figure 3.11). Mass swelling ratio

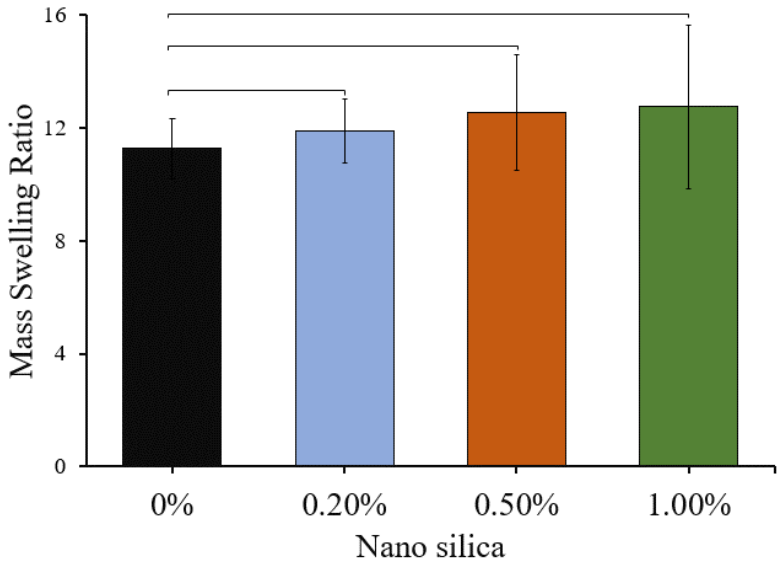

Figure 3.11 Effect of nanosilica on mass swelling ratio was investigated. Mass swelling ratio of 5% pristine GelMA and hybrid GelMA with various concentration of nanosilica (n=5).

of 5% pristine GelMA was measured as 11.25 ± 1.05. Hybrid GelMA with 0.2%, 0.5%, and 1% nanosilica increased the mass swelling ratio as 11.90 ± 1.13, 12.60 ± 2.05, and 12.75 ± 2.9 respectively which was not noteworthy. Mass swelling ratio represents the porosity of the

hydrogels. Increasing the mass swelling means the increasing of the pores. However, nanosilica did not change the hydration parameter of the pristine GelMA. One possible reason could be the nanosilica were hydrophobic.

3.4 Cell Viability of GelMA Composites

3.4.1 GelMA with Micro Bentonite

Although micro bentonite did not increase the toughness of the GelMA hydrogels, cell viability tests were done to ensure whether the particles were toxic to the cells. As it was planned that micro size would be reduced in nano size and used in GelMA. Therefore, 2D cell culture was applied to check the cell viability. 5% w/v GelMA was crosslinked in well plate and 3T3 fibroblast cells were seeded on the surface of the hydrogel. Similarly, concentrations of 0.1%, 0.2%, 0.5%, and 1% w/v of micro bentonite were dispersed and crosslinked with GelMA and 3T3 fibroblast cells were seeded on the surface of the hybrid hydrogels. All the images of figure 3.12 were taken at day 3 after the cells had been seeded on the hydrogels. Figure 3.12 showed that most of the cells were attached to the surface of the hydrogels and they were elongating. That gives the idea that the material used in the hydrogels were not cytotoxic to the cells. To be more certain about the cellular behabior on micro bentonite, another experiment was conducted. Cells were cultured in the petridishes with cell media (DMEM-Eagle medium, Thermo Fisher) and 0.1%, 0.2%, 0.5%, 1% w/v micro bentonite were added in the media and then cells were seeded on them (figure 3.13). After the first day, the cells were well attached on the surface of the petridish without any bentonite. Cells also got attached with the sample where 0.1% bentonite were added to the medium. Same went to the other concentration of bentonite. The cells were observed to be attached on the surface of the petridishes even though the particles were present. This phenomenon indicated that micro bentonite partices were not directly cytotoxic to the cells.

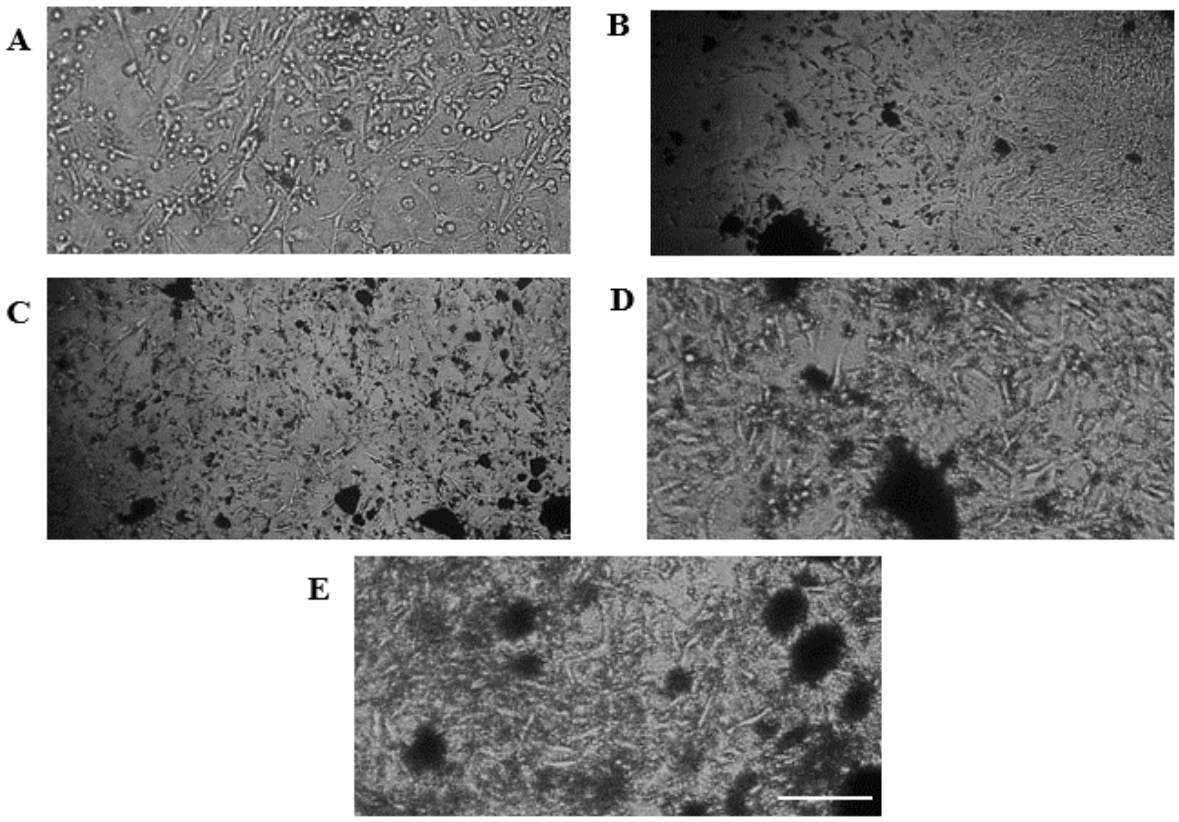

Figure 3.12 2D bright view image 3T3 cells on GelMA and different concentrations of micro bentonite with GelMA at day 3. (A) 5% GelMA with 0% micro bentonite. (B) 5% GelMA with 0.1% micro bentonite. (C) 5% GelMA with 0.2% micro bentonite. (D) 5% GelMA with 0.5% micro bentonite. (E) 5% GelMA and 1.0% micro bentonite. Scale bar = 50 µm.

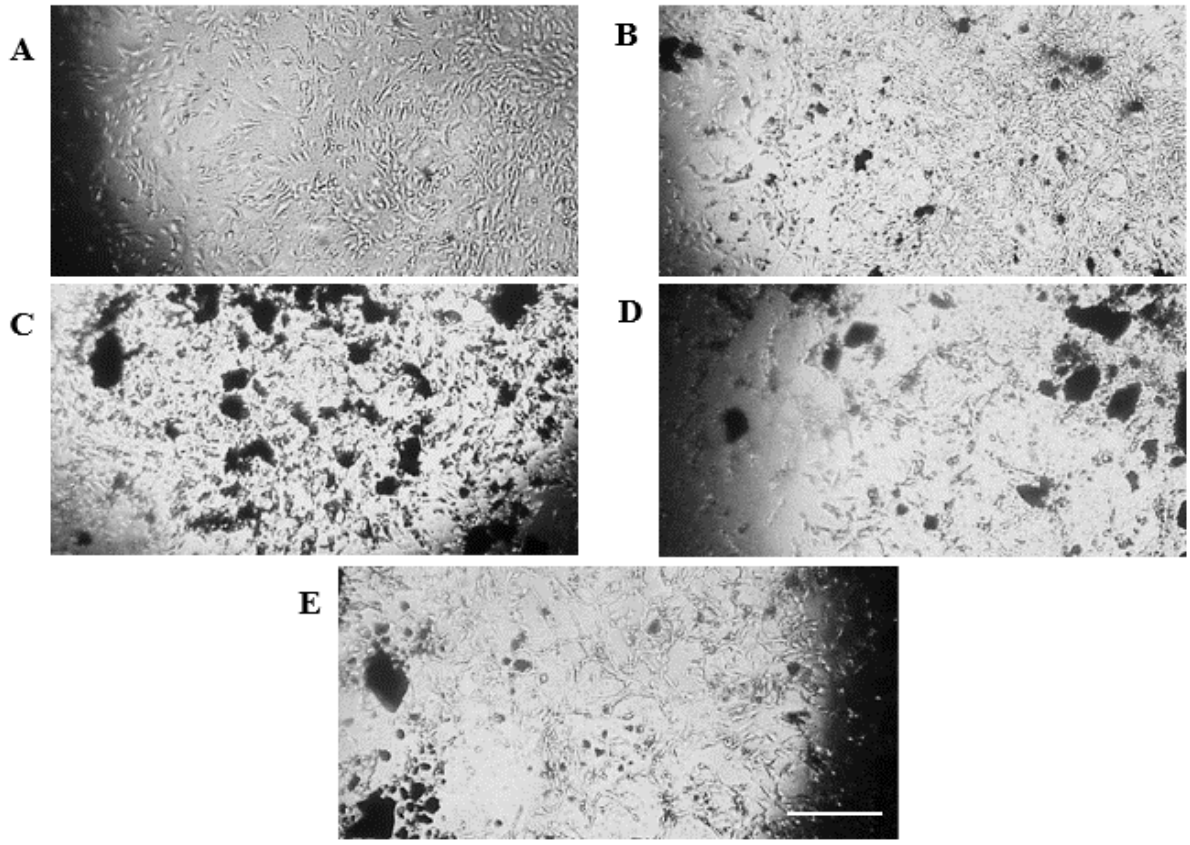

Figure 3.13 Interaction of 3T3 fibroblast cells with various concentration of micro bentonite at day 1. (A) 0% micro bentonite. (B) 0.1% micro bentonite (C) 0.2% micro bentonite. (D) 0.5% micro bentonite. (E) 1.0% micro bentonite. Scale bar = 50 µm.

3.4.2 GelMA with Nanosilica

Nanosilica observed to increase the compressibility of the GelMA by two folds. So, cell viability tests were done to ensure whether the particles were toxic to the cells. Therefore, 2D cell culture was applied to check the cell viability. 5% w/v GelMA was crosslinked in a well plate and 3T3 fibroblast cells were seeded on the surface of the hydrogel. Similarly, concentrations of 0.1%, 0.2%, 0.5%, and 1% w/v of nanosilica were dispersed and crosslinked with GelMA and 3T3 fibroblast cells were seeded on the surface of the hybrid hydrogels. All the images of figure 3.14 were taken at day 3 after the cells had been seeded on the hydrogels.

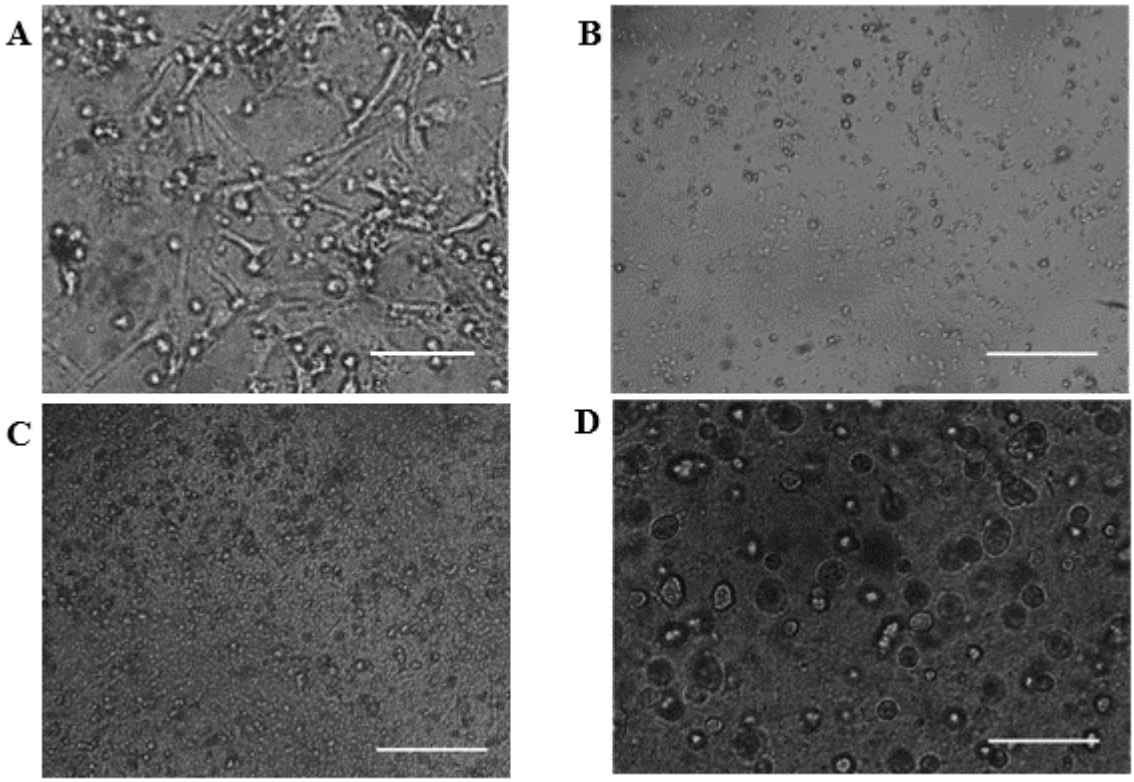

Figure 3.14 2D bright view image 3T3 cells on GelMA and different concentrations of micro bentonite with GelMA at day 3. (A) 5% GelMA with 0% nanosilica, scale bar = 50 µm. (B) 5% GelMA with 0.2% nanosilica., scale bar = 50 µm. (C) 5% GelMA with 0.5% nanosilica, scale bar = 50 µm. (D) 5% GelMA with 1% nanosilica, scale bar = 50 µm.

Most of the cells were attached on the surface of pristine GelMA and they were elongating. However, cells on the surface of GelMA containing different concentration of nanosilica did not attach and tend to die. Therefore, it was concluded that material in hybrid silica-GelMA was cytotoxic to the cells. To be more certain about the cellular behabior to nanosilica, another experiment was conducted. Cells were cultured in the petridishes with cell media (DMEM-Eagle medium, Thermo Fisher) and 0.2%, 0.5%, 1% w/v nanosilica were added in the media and then cells were seeded on them (figure 3.15).

After the first day, the cells were well attached on the surface of the petridish without any nanosilica. However, cells did not get attached with the sample where 0.1% nanosilica were added

to the medium. Same happened to the other concentration of nanosilica. This phenomenon indicates that nanosilica partices are directly cytotoxic to the cells.

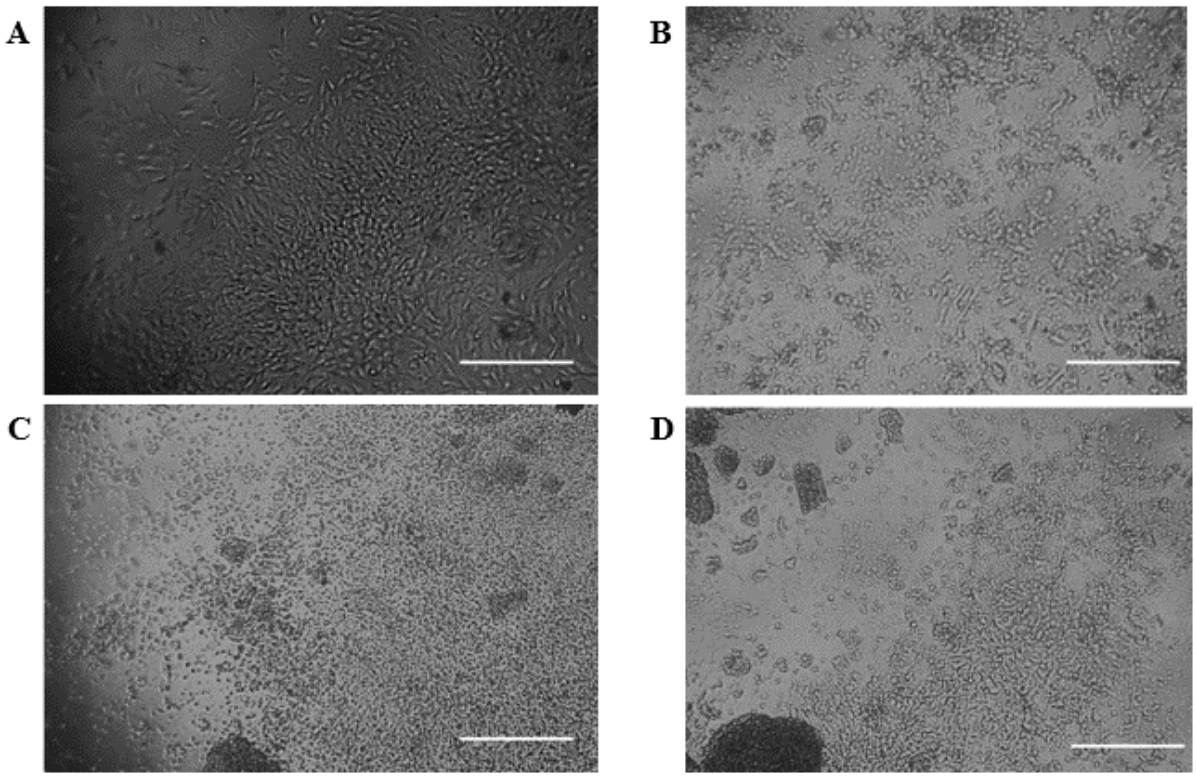

Figure 3.15 Interaction of 3T3 fibroblast cells with various concentration of nanosilica at day 1. (A) 0% nanosilica, scale bar = 50 µm. (B) 0.2% nanosilica, scale bar = 50 µm. (C) 0.5% nanosilica, scale bar = 50 µm. (D) 1% nanosilica, scale bar = 50 µm.

3.5 Summary

In this chapter, two different types of particles with GelMA were studied. The first batch of bentonite clay obtained from the Geotechnical Lab was found to be the in micro size. This batch of micro bentonite did not conjugate with the GelMA polymer properly exhibitng decreasing the mechanical properties of GelMA. However, these particles showed non toxicity to the fibroblast cells. To study the effects of nano size partices to the GelMA, nanosilica were infused to the

polymer thus increasing the mechanical properties of GelMA. Nevertheless, the nanosilica did not show compatability with the mammalian cells.

Chapter 4: Crosslinkable and Cell Viable GelMA with Nanobentonite

In chapter 3, it has been clear that GelMA are highly likely to interact with nano particles rather than micro particles. Also, nanosilica was found to be responsible for the necrosis (cell death caused by external factors). Whereas, micro bentonite was cell viable. Equipped with these knowledge, nanobentonite was synthesized and programmed to crosslink with GelMA. Therefore, this chapter aims to the design and characterization of crosslinkable and cell viable GelMA with nanobentonite.

4.1 Introduction

The challenge of tissue engineering is to resemble the essential microenvironment and complex tissue architecture to control the formation and function of the cells and tissues [59]. Therefore, well designed biomaterial that can control chemical, physical, and electrical properties of tissues are of interest for biomedical engineers. Due to the chemical and physical similarity of ECM, hydrogels are extensively used in different tissue engineering processes [133]. Over the last decade, new applications of hydrogels have emerged, particularly in stem cell engineering, immunomodulation, cellular and molecular therapies, and cancer research [61], [62]. Most of these applications demand multiple functionalities of the hydrogel network and dynamic interactions between the surrounding matrices and the cells [62]. A range of nanoparticles such as carbon-based nanomaterials CNTs, graphene, nano diamonds), polymeric nanoparticles (polymer nanoparticles, dendrimers, hyperbranched polyesters), inorganic/ceramic nanoparticles (HA, silica, silicates, calcium phosphate), and metal/metal-oxide nanoparticles (gold, silver, iron-oxide) are combined with the polymeric network to obtain nanocomposite hydrogels. These nanoparticles physically or covalently interact with the polymeric chains, and result in novel properties of the

nanocomposite network [64], [65], [66].

Hydrogel rigidity is most commonly modulated by controlling the crosslinking density of the polymer network *via* adjustments of monomer concentration and the ratio of monomer to crosslinker [134]. However, varying the crosslinking density inadvertently affects the hydrogel toughness, *i.e.* the ability to withstand applied mechanical energy without fracture, due to the correlation between rigidity and toughness of polymeric networks. Increasing the crosslinking density to enhance rigidity often results in brittleness, while decreasing the crosslinking density to reduce the rigidity leads to structural weakness [34], [35]. Thus, it is challenging to improve the toughness of hydrogel while maintaining rigidity. The rigidity of hydrogel is critical to some tissues particularly bone tissue as rigid scaffold is required to maintain cell proliferation in osseous tissue. Even though bone has the impressive ability to heal itself after major injuries, it still needs developing assistance to promote healing of reluctant defects [116]. To overcome these complexities, researchers have been focusing on nanocomposite hydrogels with different inorganic material for the past few years.

Since the discovery of isolated graphene, it has been used to reinforce the hydrogel and with that dimensionality of the reinforcing material has become known to be the most influential properties [135], [136]. This discovery sparked for the search of the new 2D nanomaterials and in the last few years many of them has come in existence namely synthetic silicate clays, layered double hydroxides (LDHs), transition metal dichalcogenides (TMDs), and transition metal oxides (TMOs) [137]. As 2D nanoparticles have at least one dimension less than 100 nm, it provides unique properties that produce high surface to volume ratio and anisotropy. These properties open up the possibilities for diversified applications in terms of drug delivery, imaging, tissue engineering, and biosensors [138], [139]. Therefore, being one of the thinnest materials, 2D

nanoparticles possess the highest specific surface areas which form charges on the surface of these particles thus create interactions among other materials on a small scale.

Due to the robust nature of 2D nanoparticles, they have been extensively investigated for drug release kinetics as they can adsorb a large numbers of drug molecules. And, the thinness of 2D nanoparticles has promised to improve the mechanical properties required for particular tissue engineering. Moreover, the unique shape of the 2D nanoparticles is breaking the boundaries for biosensing and gene sequencing as the thinness of these molecules respond well to external signals such as light which is instrumental for optical therapies including imaging application, photothermal therapy (PTT), and photodynamic therapy (PDT). Even though the emergence of the 2D nanoparticles has promised significant development in tissues engineering, their physiological interactions with living tissues in terms of particle shape and size, manufacturing impurities, and protein and immune interactions are yet to be understood [137].

The scope of the study is focused on the bentonite clays which have been in use for different medicinal purposed for few decades as antacids and topical creams, but recently their roles in biomedical application have put into investigation [91]. Tissue engineers have typically used layered silicates as 2D clay nanoparticles that are 10-100 nm in diameter and about 1 nm in thickness. The layered structure has distinct feature as negative surface charge propagates on each face of the particle and a positive charge on the edges which help the particles to possess high drug loading capacity, aqueous stability, shear thinning characteristics, and enhanced cell-nanoparticles interactions [91]. Kaolinite, palygorskite, sepiolite, and the smectites (laponite, montmorillonite, saponite, and hector rite) hold the layered structure for 2D nanoparticles [59], [140]–[143]. Among them, researchers investigate smectites extensively as these are composed of a metal cation layer sandwiched between two tetrahedral silica sheets, a 2:1-layer conformation. These nanoparticles

increase the interactions with other molecules as they have weak negatively charged surface caused by cationic substitution on the surface and consequently a net positive charge gets created on the edge of each nanoparticle. This process causes the delamination of the smectite nanoparticle which increases the surface area and nanoscale interactions with other molecules [132], [144].

In this study, an injectable osteoinductive collagen-based nanobentonite matrix was developed for bone tissue engineering. Collagen can form hydrogel naturally which is capable of imitating ECM due to the presence of cell-binding properties RGD and collagen can be modified to form covalently crosslinked hydrogels that generates tissue-like mechanical properties [32], [145], [146], [97]. The distinct characteristics of nanobentonite have the ability to stimulate strong interactions with a collagen-based matrix (gelatin) to form self-assembled structure. Gelatin and nanobentonite constitute crosslinked and stable network upon the exposure of the UV radiation (Figure 4.1). It has hypothesized that gelatin incorporated with nanobentonite will impart significant control over the mechanical and physical properties of hydrogel due to the strong interactions among the network of collagen and nanobentonite matrix. Furthermore, gelatin based hydrogel impregnated with nanobentonite stimulates ECM for the regeneration of bone tissue. Even though a significant advancement in the field of the treatment of bone diseases has occurred recently, the challenges of musculoskeletal tissue engineering still remain. Our strategy with the design of growth-factor free approach of the new biomaterial indicates a promising bioactivity in bone tissue engineering.

4.2 Materials

4.2.1 Nanobentonite

The nanobentonite used in this study had been produced in the geotechnical laboratory at the

University of British Columbia, Okanagan campus [58]. The nanobentonite used in this study was derived from the Wyoming bentonite (a type of sodium bentonite) which exhibited the characteristics of low hydraulic conductivity, self-sealing capacity and swelling characteristics [58]. It constituted of about 70 % montmorillonite content along with quartz and illite. As per [147], the major component of bentonite consists of montmorillonite which has a shape like flakes forming monoclinic crystal having lateral dimension ranging from 1000 Å to 5000 Å and thickness of 10 Å to 50 Å. In terms of minerology, montmorillonite is combined of silica tetrahedrons sheet and aluminum or magnesium octahedron sheet [147]. The average particle size of Wyoming bentonite clay happened to be within the range of 15 to 20 μm. One study (27) found that the Wyoming bentonite clay showed higher specific surface area (750 m^2/g), cation exchange capacity (76 meq/ 100g), absorption capacity (7 to 10 times of its own volume) and swelling potential (18 times of dry volume). The specific gravity and refractive index was found 1.74 and 1.48 to 1.53, respectively [148].

The nanoparticles from the Wyoming bentonite clay was extracted and it had been reported by Sarkar et al. (2016). It has been reported that the nanobentonite has the composition of 72.3 % montmorillonite, 6.9% anorthite, 10.4% illite and 10.4 % quartz [58]. Sarkar et al. (2016) also formulated the chemical composition from the energy dispersive spectroscopy (EDS) which consisted of Oxygen (O), Sodium (Na), Magnesium (Mg), Aluminium (Al), Silicon (Si), Sulphur (S), Chlorine (Cl), Potassium (K), Calcium (Ca) and Iron (Fe). And, they also hypothesized that the chemical formula of the nanobentonite is similar to the sodium based smectite mineral of $((Na,Ca)_{0.33}(Al,Mg)_2(Si_4O_{10})(OH)_2 \cdot nH_2O)$. They found that the size of the 92% nanobentonite was less than 100 nm and all the particles were below 140 nm.

4.2.2 Gelatin Methacrylate (GelMA)

The process how the Gelatin Methacrylate hydrogel (GelMA) was synthesized had been reported previously [32]. In short, the process involved of dissolving 5 g gelatin in 50 ml dimethyl sulfoxide solvent at 50 °C with stirring. Then, 0.3 g 4-dimethylaminopyridine (DMAP) was added to the mixture and kept stirred to dissolve. Subsequently, 2ml of glycidyl methacrylate was added to the mixture, and the mixture was kept stirred for two days at 50 °C. Then, the mixture was dialyzed with reverse osmosis (RO) water at room temperature for five days. The water was changed twice a day. After dialysis, the sample was freeze-dried via lyophilization. Freeze dried GelMA macromers were mixed at a concentration of 7% (w/v) into diluted PBS containing 0.5% (w/v) Irgacure 2959. All the materials we used above were purchased from Sigma Aldrich, St. Louis, MO, USA.

4.2.3 Fabrication of Nanocomposites (GelMA with nanobentonite)

The nanocomposite was fabricated in hope to have a desired combination of tunable structure and bioactivity characteristics. The prepolymer GelMA solution was processed as described above and then 0.1, 0.2, and 0.5 w/v% nanobentonite were measured by a precision balance (Sartorius, Mississauga, ON, Canada). A PBS solution was of different concentration of nanobentonite and 0.5% (w/v) photoinitiator by a precision balance (Sartorius, Mississauga, ON, Canada). A probe sonicator (Vir Sonic 100, Vir Tis) was used to disperse the nanobentonite for 15 minutes in the solution with photoinitiator. Afterwards, the nanoparticles solution was mixed with GelMA prepolymer solution and the nanoparticles in the solution were again dispersed with a sonicator probe for 15 minutes. Finally, a vortex machine (VWR Analog Vortex Mixer) was used for 30 minutes to mix the solution well, Then, the prepolymer solution was exposed under UV irradiation

to create nanocomposite hydrogel. The conjugated pristine GelMA and nanocomposite hydrogels are presented in sketch at figure 4.1.

4.3 Characterization of Physical Properties

To test mechanical properties of both pristine GelMA and GelMA incorporated with nanobentonite (nanocomposite), 5ml of each prepolymer solution was measured by a pipette and poured into a petri dish of 60 mm by 15 mm and they were exposed under ultra violet (UV) irradiation for 5 min to crosslink the hydrogel. Three cylindrical specimens were punched out (7.82 mm in diameter) from pristine GelMA and nanocomposite hydrogel. The elastic modulus of each sample was tested using a mechanical testing system (MACH-1^{TM} V500C, Biomomentum, Laval, QC, Canada). The elastic modulus was determined from the slope of the linear region between strains from 5% to 15%.

Mass swelling ratio was also tested for all the samples. 20 cylindrical specimens were prepared using the same method as described above, the residual liquid of the samples was removed with Kim Wipes. The weight of swollen specimens was measured by a precision balance (Sartorius, Mississauga, ON, Canada). After that, these samples were lyophilized at −40 °C for five days to determine the dry weight of the samples. The mass swelling ratio was determined by the following formula:

$$\text{Mass swelling ratio} = \frac{\text{swollen weight of the sample}}{dry\ weight\ of\ the\ sample} \quad (1)$$

The microstructure of the samples was monitored by coating them with 10 nm of gold–palladium (Au–Pd) alloy using sputtering. SEM was used to take images of the microstructure of each type of mixture and to analyze the elemental distribution of the nanoparticles,

nanocomposites and pristine GelMA. FT-IR of the GelMA, nanobentonite, and GelMA impregnated with nano bentonite was measured using a Shimadzu IRPrestige-21 device. The samples were prepared as powdered form after lyophilization as powdered samples were commonly used for Fourier transform infrared spectra [149], [150]. The FT-IR spectra were recorded in the range 400 to 4000 cm^{-1} infrared spectrum at 4 cm^{-1} in 1-minute accumulation around 2100 cm^{-1} peak-to-peak.

4.4 Assessment of Cell Viability

To assess the new biomaterial is biocompatible, the cell viability of Pristine GelMA and nanocomposite hydrogels were checked with various concentration of nanobentonite. After crosslinking the hydrogels on petri dishes, the NIH 3T3 fibroblast human cells were seeded on the surface of the hydrogels. After 5 days, the samples were treated with a live/dead assay (Biotium, Hayward, CA, USA) for 60 min. Afterward, the assayed samples were observed under a confocal fluorescent microscope (FV1000, Olympus, Tokyo, Japan) to check the long-term cell viability.

To capture the microscopic images, 10x objective and two fluorescent channels and one phase contrast channel were used. Sequential imaging modes were used to take groups of confocal fluorescent images with a 20μm step in the Z direction to avoid crosstalk between laser signals. Fluoview ASW software (version 3.1a, Olympus, Tokyo, Japan) was used to stack the fluorescent and phase contrast images taken by the microscope. The taken images were converted by the microscope to 16-bit gray value format to analyze the cell viability and the cell number was counted with particle counting function (Otsu Method) in ImageJ (NIH, Bethesda, MD, USA). Finally, the cell viability was calculated by the following formula:

$$\text{Cell viability} = \frac{number\ of\ live\ cells}{number\ of\ all\ cells} \quad (2)$$

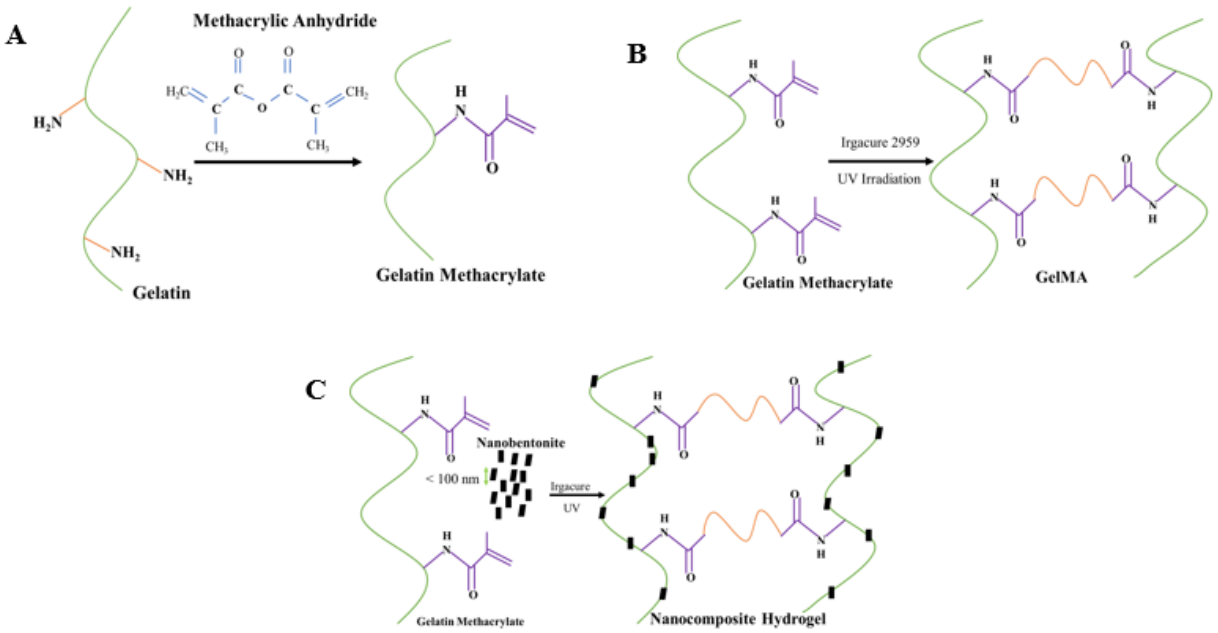

Figure 4.1 Schematic of the formation of GelMA and hybrid GelMA. (A) Gelatin Methacrylate. (B) GelMA hydrogel. and (C) nanocomposite i.e. nanobentonite with GelMA hydrogel.

4.5 Statistical analysis

One-way analysis of variance (ANOVA analysis) function in MS Excel 2016 (Microsoft Corporation, Redmond, Washington, USA) was used to statistically analyze the data of mechanical properties, swelling ratio, and cell viability. Results are shown as an average ± standard deviation.

4.6 Results and Discussion

The experimental data were analyzed and discussed in the following sections. At first, it was checked whether the nano particles could bond with the polymer network. Then, the mechanical properties such as compressibility and swelling ratio were checked. Finally, the cell viability was investigated through live/dead assay in 2D.

4.6.1 Crosslinking Nanobentonite with GelMA

It was hypothesized that nanobentonite had the similar chemical formula similar to sodium based smectite mineral of $((Na,Ca)_{0.33}(Al,Mg)_2(Si_4O_{10})(OH)_2 \cdot nH_2O)$. It is evident that the nanobentonite has the hydro-oxide ions bonded with other elements which has the high aspect ratio (less than 100 nm in diameter and thinner thickness) (Figure 4.2). Consequently, a strong interaction was expected between nanobentonite and gelatin based polyampholytic hydrogel [59]. It was known that amine groups present on the gelatin backbone has to be replaced by the methacrylate group to acquire stable, biodegradable and cell viable hydrogel GelMA [32], [145], [146], [97]. Therefore, it was assumed that bonding between nanobentonite and GelMA was possible. Prepolymer GelMA solution was cross-linked to GelMA hydrogel in the presence of a photoinitiator under UV irradiation. 0.1, 0.2, and 0.5% w/v of the nanobentonite was prepared to covalently bond with GelMA for the purpose of physical and biological characterization. The presence of nanobentonite was determined within the gelatin network after cross-linking via FT-IR as shown in figure 4.3. Nanobentonite had the peak between 1000 cm^{-1} and 1200 cm^{-1} due to the presence of Si-O-Si and GelMA hydrogel had the defined amine peaks near 1540 cm^{-1} and 1650 cm^{-1}. During the analysis,

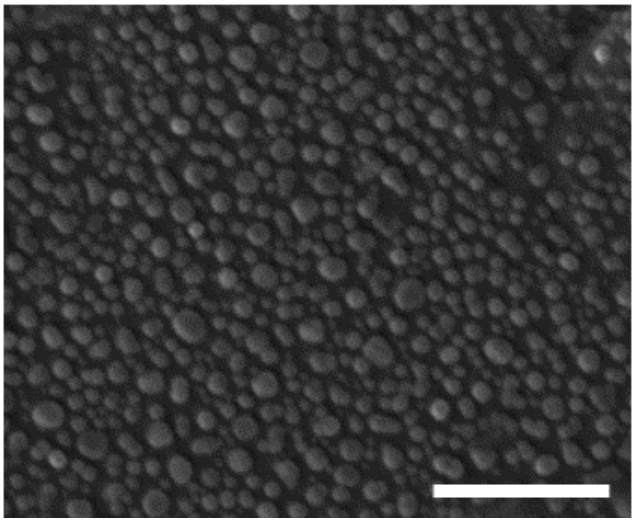

Figure 4.2 SEM image of nanobentonite. Scale bar = 500 nm.

the nanocomposite (GelMA crosslinked with nanobentonite) under FT-IR had both Si-O-Si and amides peaks which confirmed the nanobentonite was bonded with GelMA covalently.

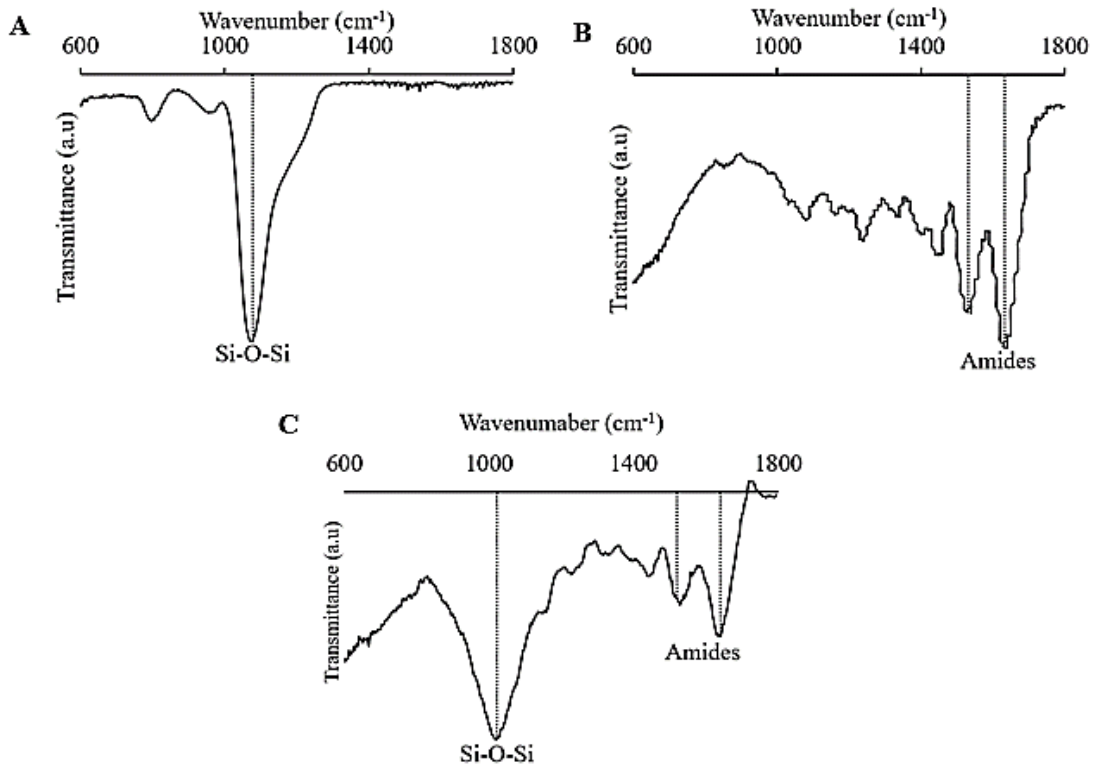

Figure 4.3 FT-IR spectra of hybrid hydrogel. (A) Bentonite nanoparticles with Si-O-Si peak. (B) Pristine GelMA with amides peaks. (C) Hybrid nanobentonite GelMA with both Si-O-Si and amides peaks.

The mass swelling ratio of the hydrogels was also inspected as this property gives an insight about surface properties and mobility and solute diffusion [68]. Swelling ratio also indicates the porosity of hydrogels which is important for cellular behavior, as the cellular infiltration and distribution of cells depend on the size of the pore of hydrogel network [151], [152]. The calculated mass swelling ratio of pristine 7% w/v GelMA and nanocomposites of different concentrations was showed in figure 4.4. The higher 0.5% w/v nanobentonite concentration in the GelMA gave lower mass swelling ratio which was 7.47 ± 0.21. There was no significant change in swelling

ratio among pristine GelMA and 0.1, 0.2% nanocomposite GelMA which were 9.24 ± 0.21, 9.25 ± 0.36, and 9.33 ± 0.66. The mass swelling ratio was significantly decreased at 0.5% nanocomposite. Lower mass swelling ratio meant high interaction between the particles and the polymer [116].

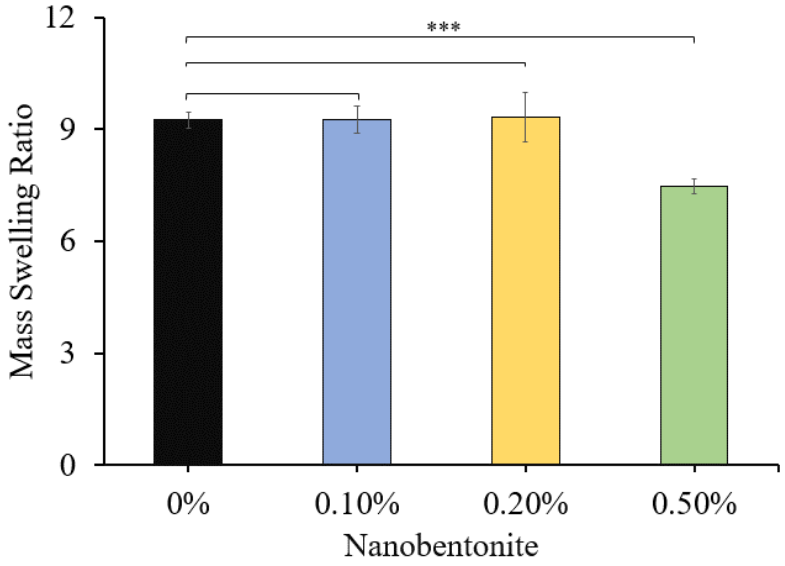

Figure 4.4 Effect of nanobentonite on mass swelling ratio was investigated. Mass swelling ratio of 7% pristine GelMA and hybrid GelMA with various concentration of nanobentonite (*p<0.001, n=5).**

From the previous study, it was known that the Gel hydrogels showed a uniform and highly interconnected network [107]. But, the addition of nanobentonite increased the pore size of the nanocomposite while compared with the pristine GelMA (figure 4.5). Pristine GelMA displayed a pore size ranging from 5.1 to 12.1µm, whereas the addition of 0.1% w/v nanobentonite did not change the pore size ranging from 6.1 to 12.3µm. 0.2% w/v addition of nanobentonite increased the pore size ranging between 26.2 to 33.4µm. And, 0.5% w/v addition of nanobentonite increased the pore size about 6 folds ranging between 43 to 56µm. Previously, it had been shown that the physical reinforcement of the hydrogel network by nanoparticles resulted in smaller pore size

[153], [154]. Therefore, the increase of the pore size in addition of nanobentonite indicated the enhanced correlation between the nanoparticles and GelMA. The formation of larger voids resulted from local condensation of the polymer fraction in the hydrogel [116]. While investigating the microscopic images (figure 4.5), we found that no visible or very little agglomeration of nanoparticles occurred in polymeric network. The elemental analysis of nanobentonite, pristine GelMA and nanocomposite hydrogels using EDS also confirmed the elements like silicon (Si), aluminum (Al), magnesium (Mg) were present in nanocomposite hydrogels. These elements were

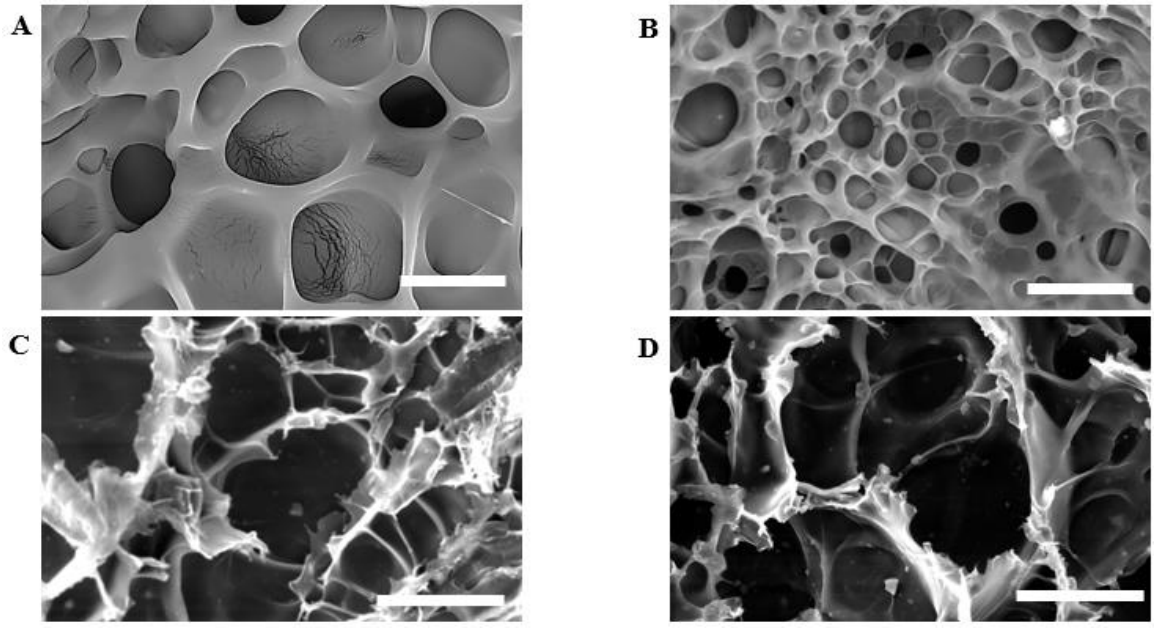

Figure 4.5 Micro structure of GelMA and hybrid GelMA after adding nanobentonite. (A) 7% GelMA, scale bar = 20 µm. (B) 7% GelMA with 0.1% nanobentonite, scale bar = 20 µm. (C) 7% GelMA with 0.2% nanobentonite, scale bar = 50 µm. (D) 5% GelMA with 0.5% nanobentonite, scale bar = 50 µm.

not found in the pristine GelMA which indicated that these elements were coming from nanobentonite resulting a proper interaction between GelMA and nanoparticles (figure 4.6).

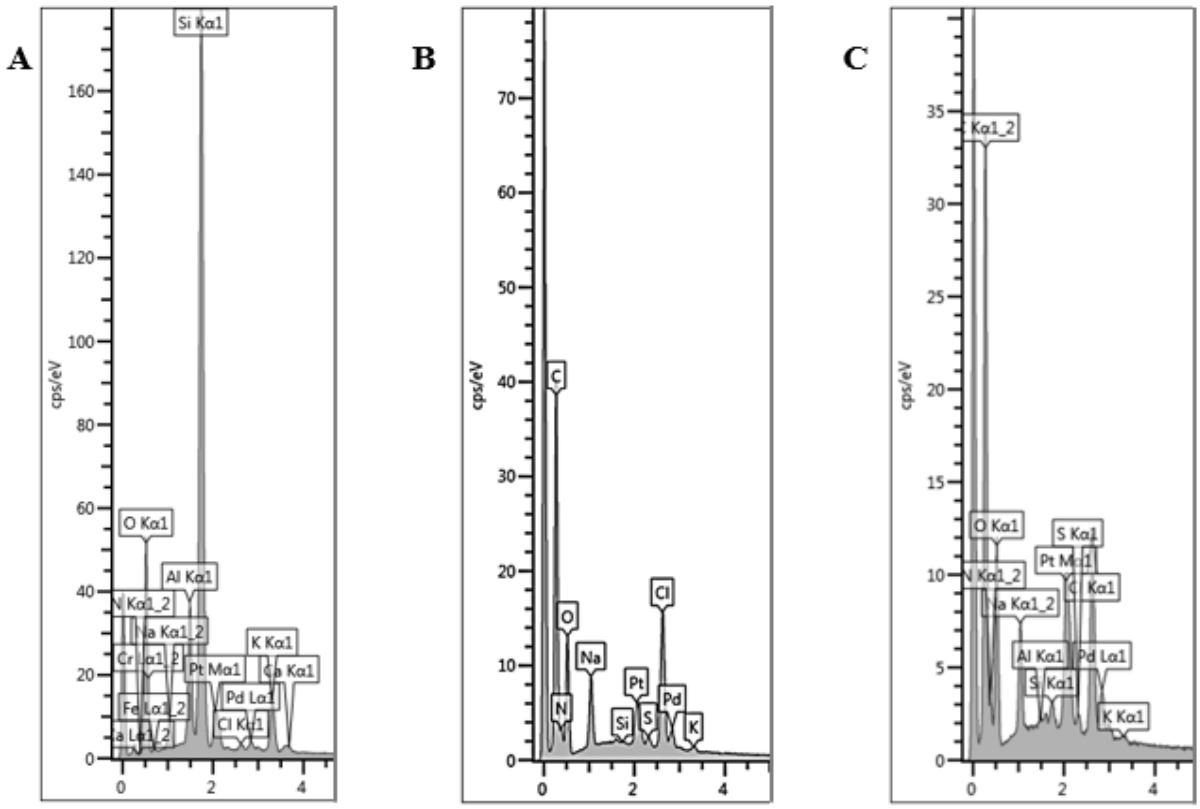

Figure 4.6 EDS of hybrid hydrogel. (A) Bentonite nanoparticles with Al, Na, Si, Mg, and Ca peaks. (B) Pristine GelMA with N, C, O, Cl, Na peaks. (C) Hybrid nanobentonite GelMA with elements both from nanobentonite and GelMA hydrogel.

4.6.2 Enhancing Mechanical Stiffness

Crosslinked nanobentonite with GelMA increased the mechanical stiffness of the hydrogel. To test the toughness of the hydrogels physically, the gels were tried to cut through with a knife, the pristine GelMA was broken apart very easily while the nanocomposite of 0.5% bentonite showed significant stability under stress (figure 4.7). Subsequently, the hydrogel samples were subjected under uniaxial compression testing to quantify the compression modulus. The results presented the increase of stress with an increase in strain (figure 4.8). The initial linear region ranging from 5% to 15% mm/mm strain was taken into consideration to calculate the elastic modulus of the hydrogels (figure 4.8). The modulus of pristine GelMA was found to be 7.1 ± 0.91 kPa which was

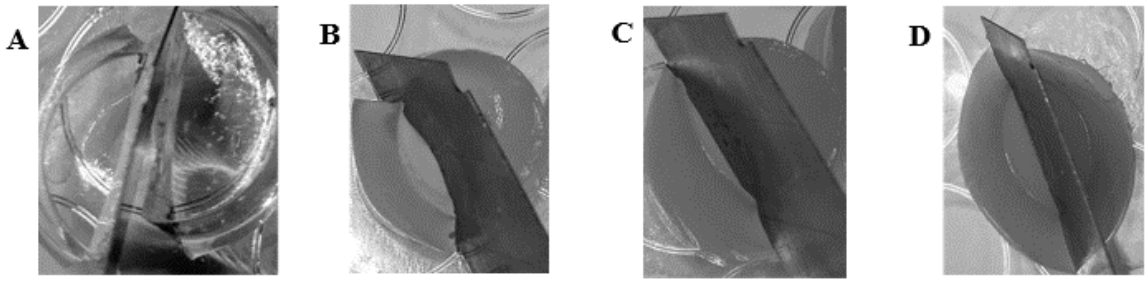

Figure 4.7 Physical Testing of Hybrid GelMA with Nanobentonite. (A) 7% pristine GelMA. (B) 7% GelMA with 0.1% nanobentonite. (C) 7% GelMA with 0.2% nanobentonite. (D) 7% GelMA with 0.5% nanobentonite.

supported by the previous reports [71], [155]. Small amount of nanobentonite was added to increase the elastic modulus. The addition of 0.1, 0.2, and 0.5% nanobentonite resulted in an increase of elastic modulus to 9.9 ± 0.56, 27.25 ± 0.31, 41.82 ± 1.3 kPa, respectively (figure 4.8). The addition of small amount of nanobentonite increased the elastic modulus by 6- fold due to the enhanced nanoparticle-polymer interaction. The addition of 0.5% nanobentonite also could resist

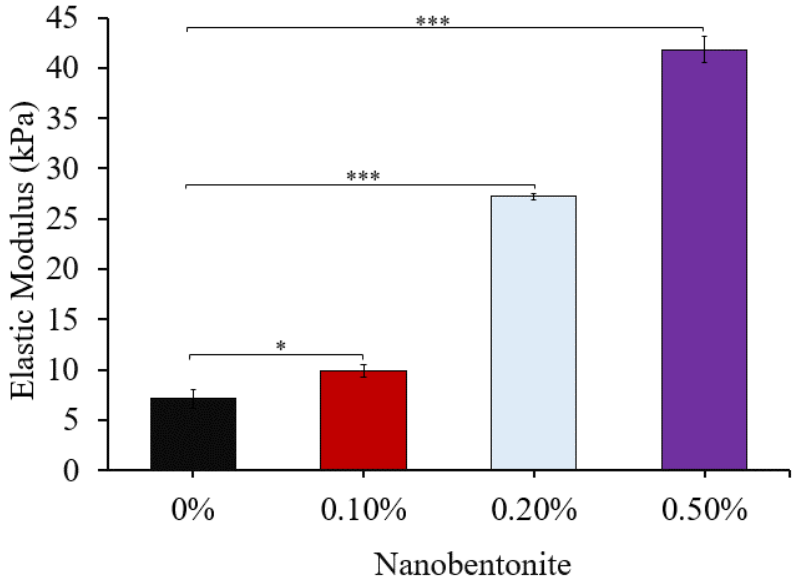

Figure 4.8 Characterization of the mechanical properties of nanobentonite hybrid GelMA: Determining the elastic modulus of 7% GelMA and various concentration of nanobentonite with GelMA (*p<0.05, ***p<0.001, n=5).

a 10-fold increase of stress at 28% strain compared with the pristine GelMA (figure 4.9) In previous studies, different kinds of nanoparticles had been used to increase the elastic modulus of GelMA but those nanocomposites showed very minimal increase in modulus [71], [107]. On the other hand, covalently conjugated nanoparticles with GelMA can increase the elastic modulus of hydrogels [112]. In this study, nanoparticles were covalently cross-linked with GelMA hydrogel and this process increased the elastic modulus of GelMA significantly. As the previous study [33] suggested, the elasticity of the hydrogel polymer had the direct correlation of the growth adhesion, and proliferation of stem cells. Therefore, increasing the stiffness of the "soft gel" GelMA [32] would play a vital role in cell differentiation and proliferation.

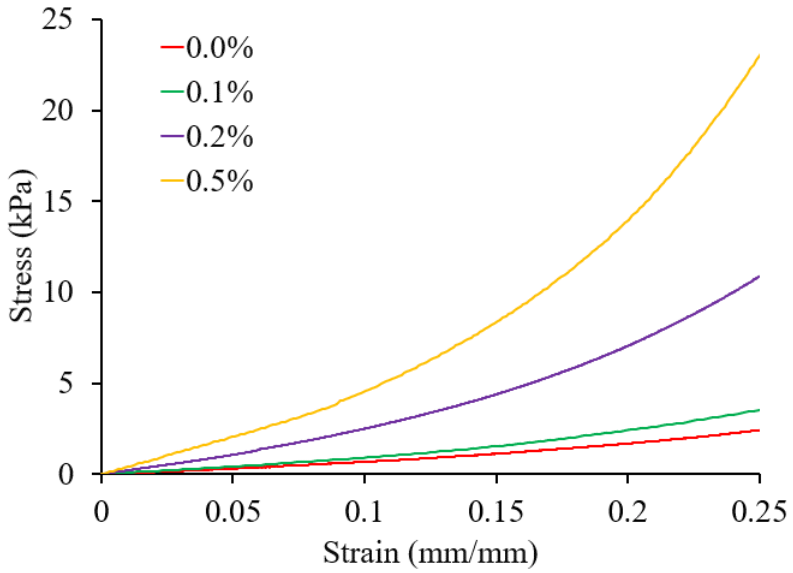

Figure 4.9 Characterization of the mechanical properties of nanobentonite hybrid GelMA: Determining the Strain-stress curve of 7% GelMA and various concentration of nanobentonite with GelMA.

4.6.3 Nanobentonite enhanced cell adhesion and proliferation

Tissue engineering requires well cell adhesion and proliferation for the biomaterial to be used as scaffold. It has been established that the gelatin is cell viable as it is a denatured protein that

contains RGD groups, which supports cell adhesion via integrins. To test the cell viability, NIH 3T3 cells were seeded on the surface of the GelMA and nanocomposites. The GelMA and nanocomposites showed early signs of cell adhesion and no significant morphological change occurred due the presence of nanobentonite (figure 4.10). After five days, the cells showed very well cell adhesion and growth indicating that the nanocomposites were cytocompatible. A previous study reported that the large pore size of hydrogels contributed the acceleration of biomolecules

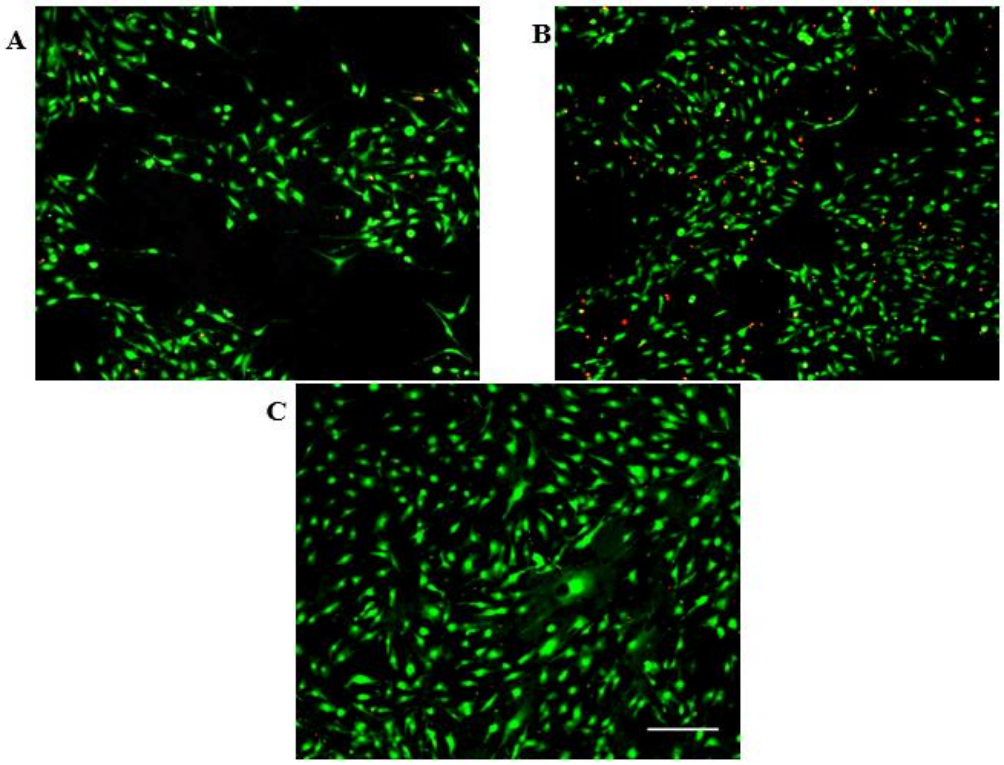

Figure 4.10 2D image of live/dead assay at day 5. (A) pristine 7% GelMA hydrogel. (B) 0.1% nanobentonite crosslinked with GelMA. and (C) 0.5% nanobentonite crosslinked with GelMA. Scale for all the images = 200 µm.

exchange thus promoting the long-term cell viability [156]. The live/dead assay on day 5, showed the cell viability of 0.5% nanocomposite was 91.03 ± 2.37% whereas the cell viability of pristine GelMA and 0.1% nanocomposite were 81.24 ± 2.31%, and 80.76 ± 1.78%, respectively (figure

4.11). No change in cell viability occurred for the 0.1% nanocomposite when compared with the pristine GelMA. In contrast, 0.5% nanocomposite exhibit better cell viability due the large pore size in the matrices. Therefore, the newly developed novel biomaterial is cell viable, biodegradable material.

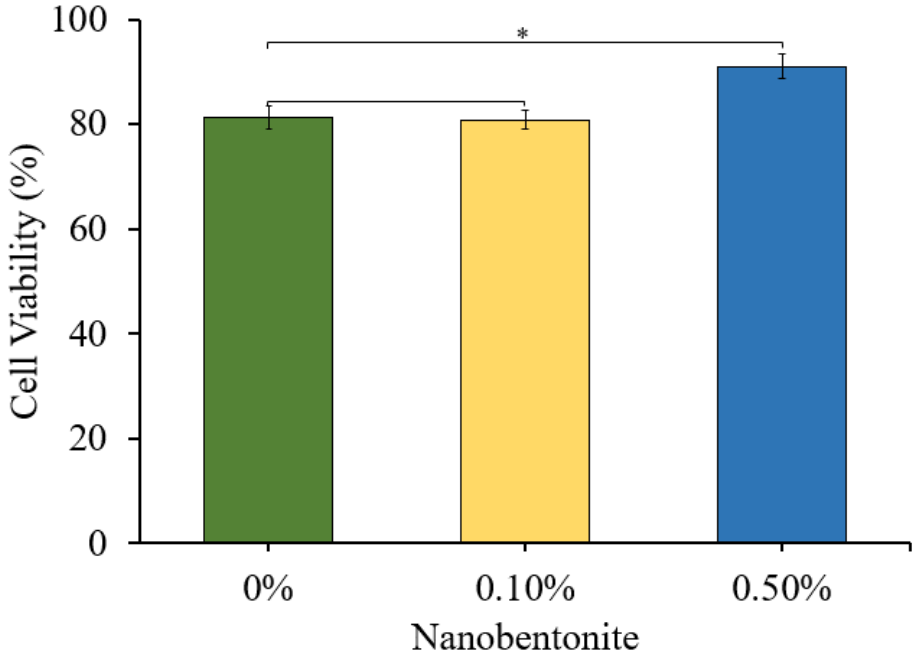

Figure 4.11 Cell viability at day 5 of pristine GelMA and nanobentonite crosslinked with GelMA, n=5, *p<0.05.

4.7 Summary

In this chapter, a novel bioactive nanocomposite hydrogel was presented. The design of the biomaterial involved the inclusion of nanobentonite in the GelMA polymeric chains covalently. Although, the study of clay nanoparticles in tissue engineering is still in primitive stage, it was clear from the experiments that this bioactive material promoted chemical interactions between nanoparticles and hydrogel chain. Because, particles in nano size tend to bond with polymers which are also in same size. Consequently, this material has a potential use in wide range of

biomedical applications, including drug delivery system, bone regeneration, regenerative medicine, therapeutics, imaging, and disease-related diagnostics. It was very likely that the GelMA hydrogel and nanobentonite interacted with each other electrostatically, thus enhancing mechanical, chemical, and biological properties of the GelMA hydrogel. Incorporation of nanobentonite increased the mechanical toughness of GelMA which promoted cellular stability in-vitro condition. The tunable mechanical properties of the nanocomposite also supported cell proliferation, differentiation, and adhesion, thus making this bioactive material as a potential nominee for the wide range of osteogenic tissue engineering application.

Chapter 5: Conclusion

5.1 Conclusions

Biomaterial is the heart of tissue engineering. Different tissues react with different biomaterial very uniquely. For example, special graft is needed for the treatment of the fractured or decayed bone tissue engineering. Natural polymers have gained popularity to use as a base material to form a graft. Using ceramic nanoparticles in the polymer graft have gained momentum to tailor the properties of the polymer as desired due to their easy availability and they also mimic the minerals found in our body. Having many potential usages, GelMA with ceramic nanoparticles have been employed to fabricate vascularized tissues, investigate cancer migration, culture stem cell in 3D microenvironments, and build *in vitro* drug screening platform. However, in bone tissue application, polymer grafts need to be tough as well as elastic. Therefore, it is desired to obtain a hybrid hydrogel which has the ability to interact with the nanoparticles resulting higher rigidity without affecting the cellular viability.

In this thesis, GelMA hydrogels had been impregnated with tree different types of clay particles both nano and micro in size to design a novel biomaterial which obtain the resilience of bone tissue. Lab grown micro size bentonite clay was first introduced with GelMA to increase its elastic modulus. But, these particles did not increase the toughness of the GelMA. However, GelMA incorporated with micro bentonite was not toxic to the NIH 3T3 fibroblast cells. Afterward, nanosilica was introduced in GelMA and these nano particles indeed raised the rigidity of the GelMA by two folds, contrarily, they were also responsible for the death of cells *in vitro.* Therefore, nanobentonite synthesized from micro bentonite was introduced as bentonite particles were not cytotoxic. First of all, well dispersed nanobentonite crosslinked with GelMA covalently. They increased the pore size of GelMA about 10 folds resulting

hospitable environments to cell growth. Nanobentonite was also responsible of 6-fold increase of mechanical stiffness of GelMA. In 2D cell culture, hybrid GelMA with nanobentonite showed enhanced cell growth and proliferation.

In summary, the objectives of the thesis were achieved through the development and demonstration of the novel biomaterial using GelMA and nanobentonite which were able to crosslink with GelMA in the presence of UV radiation. The hybrid GelMA also improved the mechanical stiffness of the pristine GelMA as well as increased the pore size of the hydrogel. The developed biomaterial enhanced the cell growth and proliferation in 2D cell culture *in vitro*. Based on the affordability of the materials of the new biomaterial, nanobentonite based nanocomposite hydrogel will be a fine choice for a variety of tissue engineering applications.

5.2 Major Contributions

A novel biomaterial is designed by adding bentonite nanoparticles with GelMA hydrogel. This was the first time, nanobentonite had been conjugated with GelMA polymers covalently opening a wide spectrum of opportunities in various biomedical applications due to its cytocompatibility with NIH 3T3 fibroblast cells. Among other tissue engineering applications, bentonite nanocomposites could be used in healing nonunion bone defects and bone fracture by providing a suitable scaffold for osteogenic cells' rapid growth and proliferation.

5.3 Future Work

Hybrid biomaterial is a rapidly developing area. There are many paths for the future research including biofabrication techniques by 3D printing and programmed self-assembly, refined

drug delivery mechanism, interaction between foreign bodies and body's immune surveillance system, and better biomimetic tissues for *in vivo* studies.

5.3.1 *In Vivo* Studies

Biomaterials are mostly examined in lab for the cell functionality and cell viability *in vitro.* However, the main goal of tissue engineering is to put the artificial tissue in the 3-dimensional live environment. 3D bioprinted tissue transplantation has been recently studied *in vivo* [157]. They reported that bioprinted skeletal muscle went through vascularization and nerve regeneration and functional muscle tissue was formed when electrical stimulation was applied. After four weeks of maturation, this tissue was able to perform as a real muscle-like tissue and could generate resistance when contracted. In the last couple of years, many *in vitro* studies have been converted into *in vivo* studies using bioprinted tissues thus enhancing the possibilities to use lab grown tissues in real life and clinical trial. Nanobentonite-GelMA hydrogel has potential to be used as bioink in a 3D bioprinter.

5.3.2 Architecture of Tissue Scaffolds

Human tissue like structures have been constructed by programmed self-assembly and 3D bioprinting so far [152], [158]. DNA strands in appropriate condition can produce self-assembly tissue structure [159], [160]. Nanobentonite-GelMA hydrogel can be used a supporting material for DNA strands based tissue formation. However, biofabrication approach is also popular technique to grow tissues in the lad in extension to the 3D bioprinting. Biofabrication provides unforeseen control to manipulate cells and biomolecules (e.g., proteins and ECM) with precise governance over composition and spatial distribution to repeat the

exact shape, structure and architecture of native tissues [31], [161]. A wide range of biomaterials can be used for the application and nanobentonite-GelMA hydrogel can be a potent biomaterial due its versatility in terms of rigidity, affordability, and biocompatibility.

References

[1] K. K. Kar, J. K. Pandey, and S. Rana, Eds., *Handbook of Polymer Nanocomposites. Processing, Performance and Application*. Berlin, Heidelberg: Springer Berlin Heidelberg, 2015.

[2] B. Sarker, S. Lyer, A. Arkudas, and A. R. Boccaccini, "Collagen/silica nanocomposites and hybrids for bone tissue engineering," *Nanotechnol. Rev.*, vol. 2, no. 4, Jan. 2013.

[3] A. Khademhosseini, R. Langer, J. Borenstein, and J. P. Vacanti, "Microscale technologies for tissue engineering and biology," *Proc. Natl. Acad. Sci.*, vol. 103, no. 8, pp. 2480–2487, Feb. 2006.

[4] M. Liu *et al.*, "Injectable hydrogels for cartilage and bone tissue engineering," *Bone Res.*, vol. 5, p. 17014, May 2017.

[5] A. Jiao *et al.*, "Thermoresponsive Nanofabricated Substratum for the Engineering of Three-Dimensional Tissues with Layer-by-Layer Architectural Control," *ACS Nano*, vol. 8, no. 5, pp. 4430–4439, May 2014.

[6] Z. Wang, R. Samanipour, K. Koo, and K. Kim, "Organ-on-a-chip platforms for drug delivery and cell characterization: A review," *Sensors Mater.*, vol. 27, no. 6, pp. 487–506, 2015.

[7] R. Dai, Z. Wang, R. Samanipour, K. Koo, and K. Kim, "Adipose-Derived Stem Cells for Tissue Engineering and Regenerative Medicine Applications," *Stem Cells Int.*, vol. 2016, pp. 1–19, 2016.

[8] C. Mandrycky, Z. Wang, K. Kim, and D.-H. Kim, "3D bioprinting for engineering complex tissues," *Biotechnol. Adv.*, vol. 34, no. 4, pp. 422–434, Jul. 2016.

[9] J. Venkatesan and S. K. Kim, “Carbon Nanotube for Bone Repair,” in *Handbook of Polymer Nanocomposites. Processing, Performance and Application*, Berlin, Heidelberg: Springer Berlin Heidelberg, 2015, pp. 511–526.

[10] C. R. M. Black, V. Goriainov, D. Gibbs, J. Kanczler, R. S. Tare, and R. O. C. Oreffo, “Bone Tissue Engineering,” *Curr. Mol. Biol. Reports*, vol. 1, no. 3, pp. 132–140, Sep. 2015.

[11] T. Yamada *et al.*, “Hybrid Grafting Using Bone Marrow Aspirate Combined With Porous β-Tricalcium Phosphate and Trephine Bone for Lumbar Posterolateral Spinal Fusion,” *Spine (Phila. Pa. 1976).*, vol. 37, no. 3, pp. E174–E179, Feb. 2012.

[12] C. R. Fischer, R. Cassilly, W. Cantor, E. Edusei, Q. Hammouri, and T. Errico, “A systematic review of comparative studies on bone graft alternatives for common spine fusion procedures,” *Eur. Spine J.*, vol. 22, no. 6, pp. 1423–1435, Jun. 2013.

[13] J. Verhaegen, S. Clockaerts, G. J. V. M. Van Osch, J. Somville, P. Verdonk, and P. Mertens, “TruFit Plug for Repair of Osteochondral Defects—Where Is the Evidence? Systematic Review of Literature,” *Cartilage*, vol. 6, no. 1, pp. 12–19, Jan. 2015.

[14] B. J. Cole *et al.*, “Outcomes After a Single-Stage Procedure for Cell-Based Cartilage Repair,” *Am. J. Sports Med.*, vol. 39, no. 6, pp. 1170–1179, Jun. 2011.

[15] J. C. Reichert *et al.*, “A Tissue Engineering Solution for Segmental Defect Regeneration in Load-Bearing Long Bones,” *Sci. Transl. Med.*, vol. 4, no. 141, p. 141ra93-141ra93, Jul. 2012.

[16] L. Ren, Y. Kang, C. Browne, J. Bishop, and Y. Yang, “Fabrication, vascularization and osteogenic properties of a novel synthetic biomimetic induced membrane for the treatment of large bone defects,” *Bone*, vol. 64, pp. 173–182, Jul. 2014.

[17] A. Berner *et al.*, “Delayed Minimally Invasive Injection of Allogenic Bone Marrow Stromal Cell Sheets Regenerates Large Bone Defects in an Ovine Preclinical Animal Model,” *Stem Cells Transl. Med.*, vol. 4, no. 5, pp. 503–512, May 2015.

[18] D. Orlic *et al.*, “Bone marrow cells regenerate infarcted myocardium,” *Nature*, vol. 410, no. 6829, pp. 701–705, Apr. 2001.

[19] S. H. Cameron *et al.*, “Delayed post-treatment with bone marrow-derived mesenchymal stem cells is neurorestorative of striatal medium-spiny projection neurons and improves motor function after neonatal rat hypoxia–ischemia,” *Mol. Cell. Neurosci.*, vol. 68, pp. 56–72, Sep. 2015.

[20] T. Dreger *et al.*, “Intravenous Application of CD271-selected Mesenchymal Stem Cells During Fracture Healing,” *J. Orthop. Trauma*, vol. 28, pp. S15–S19, Apr. 2014.

[21] J. Venkatesan and S.-K. Kim, “Chitosan Composites for Bone Tissue Engineering—An Overview,” *Mar. Drugs*, vol. 8, no. 8, pp. 2252–2266, Aug. 2010.

[22] L. Wang, R. M. Shelton, P. R. Cooper, M. Lawson, J. T. Triffitt, and J. E. Barralet, “Evaluation of sodium alginate for bone marrow cell tissue engineering,” *Biomaterials*, vol. 24, no. 20, pp. 3475–3481, Sep. 2003.

[23] J. L. Drury and D. J. Mooney, “Hydrogels for tissue engineering: scaffold design variables and applications,” *Biomaterials*, vol. 24, no. 24, pp. 4337–4351, Nov. 2003.

[24] P. Zorlutuna, N. E. Vrana, and A. Khademhosseini, “The Expanding World of Tissue Engineering: The Building Blocks and New Applications of Tissue Engineered Constructs,” *IEEE Rev. Biomed. Eng.*, vol. 6, pp. 47–62, 2013.

[25] J. Zhu and R. E. Marchant, “Design properties of hydrogel tissue-engineering scaffolds,” *Expert Rev. Med. Devices*, vol. 8, no. 5, pp. 607–626, Sep. 2011.

[26] A. S. Hoffman, “Hydrogels for biomedical applications,” *Adv. Drug Deliv. Rev.*, vol. 64, pp. 18–23, Dec. 2012.

[27] T. Nishimura, A. Hattori, and K. Takahashi, “Ultrastructure of the Intramuscular Connective Tissue in Bovine Skeletal Muscle,” *Cells Tissues Organs*, vol. 151, no. 4, pp. 250–257, 1994.

[28] K. T. Nguyen and J. L. West, “Photopolymerizable hydrogels for tissue engineering applications,” *Biomaterials*, vol. 23, no. 22, pp. 4307–4314, Nov. 2002.

[29] S. Limpanuphap and B. Derby, “No Title,” *J. Mater. Sci. Mater. Med.*, vol. 13, no. 12, pp. 1163–1166, 2002.

[30] D. W. Hutmacher, “Scaffolds in tissue engineering bone and cartilage,” *Biomaterials*, vol. 21, no. 24, pp. 2529–2543, Dec. 2000.

[31] S. V Murphy and A. Atala, “3D bioprinting of tissues and organs,” *Nat. Biotechnol.*, vol. 32, no. 8, pp. 773–785, Aug. 2014.

[32] J. W. Nichol, S. T. Koshy, H. Bae, C. M. M. Hwang, S. Yamanlar, and A. Khademhosseini, “Cell-laden microengineered gelatin methacrylate hydrogels,” *Biomaterials*, vol. 31, no. 21, pp. 5536–5544, Jul. 2010.

[33] A. J. Engler, S. Sen, H. L. Sweeney, and D. E. Discher, “Matrix Elasticity Directs Stem Cell Lineage Specification,” *Cell*, vol. 126, no. 4, pp. 677–689, Aug. 2006.

[34] R. F. Landel and L. E. Nielsen, *Mechanical properties of polymers and composites*. New York: Marcel Dekker, 1994.

[35] H. J. Kong, E. Wong, and D. J. Mooney, “Independent Control of Rigidity and Toughness of Polymeric Hydrogels,” *Macromolecules*, vol. 36, no. 12, pp. 4582–4588, Jun. 2003.

[36] M. C. Roco, “Environmentally Responsible Development of Nanotechnology,” *Environ. Sci. Technol.*, vol. 39, no. 5, p. 106A–112A, Mar. 2005.

[37] M. A. Wilson, N. H. Tran, A. S. Milev, G. S. K. Kannangara, H. Volk, and G. Q. M. Lu, “Nanomaterials in soils,” *Geoderma*, vol. 146, no. 1–2, pp. 291–302, Jul. 2008.

[38] C. L. DeCastro and B. S. Mitchell, “Nanoparticles from Mechanical Attrition,” *Nanoparticles from Mech. attrition. Synth. Funct. Surf. Treat. Nanoparticles*, pp. 1–15, 2002.

[39] F. Song, X. Li, Q. Wang, L. Liao, and C. Zhang, “Nanocomposite Hydrogels and Their Applications in Drug Delivery and Tissue Engineering,” *J. Biomed. Nanotechnol.*, vol. 11, no. 1, pp. 40–52, Jan. 2015.

[40] K.-H. Liu, T.-Y. Liu, S.-Y. Chen, and D.-M. Liu, “Drug release behavior of chitosan–montmorillonite nanocomposite hydrogels following electrostimulation,” *Acta Biomater.*, vol. 4, no. 4, pp. 1038–1045, Jul. 2008.

[41] W.-F. Lee and Y.-C. Chen, “Effect of hydrotalcite on the physical properties and drug-release behavior of nanocomposite hydrogels based on poly[acrylic acid-co-poly(ethylene glycol) methyl ether acrylate] gels,” *J. Appl. Polym. Sci.*, vol. 94, no. 2, pp. 692–699, Oct. 2004.

[42] A. M. Hawkins, C. E. Bottom, Z. Liang, D. A. Puleo, and J. Z. Hilt, “Magnetic Nanocomposite Sol-Gel Systems for Remote Controlled Drug Release,” *Adv. Healthc. Mater.*, vol. 1, no. 1, pp. 96–100, Jan. 2012.

[43] A. K. Bajpai and R. Gupta, “Magnetically mediated release of ciprofloxacin from polyvinyl alcohol based superparamagnetic nanocomposites,” *J. Mater. Sci. Mater. Med.*, vol. 22, no. 2, pp. 357–369, Feb. 2011.

[44] N. SATARKAR and J. HILT, “Magnetic hydrogel nanocomposites for remote controlled pulsatile drug release,” *J. Control. Release*, vol. 130, no. 3, pp. 246–251, Sep. 2008.

[45] Y. Jiang, B. Li, X. Chen, and M. Zhu, “Preparation and characterization of a prolonged and sustained drug delivery system: Linear polyacrylamide in poly(N-isopropylacrylamide)/clay hydrogels,” *J. Appl. Polym. Sci.*, vol. 125, no. S1, pp. E148–E156, Jul. 2012.

[46] M. KAWAGUCHI *et al.*, “Preparation of Carbon Nanotube-alginate Nanocomposite Gel for Tissue Engineering,” *Dent. Mater. J.*, vol. 25, no. 4, pp. 719–725, 2006.

[47] S. R. Shin *et al.*, “Carbon Nanotube Reinforced Hybrid Microgels as Scaffold Materials for Cell Encapsulation,” *ACS Nano*, vol. 6, no. 1, pp. 362–372, Jan. 2012.

[48] T. Wang *et al.*, “Rapid cell sheet detachment from alginate semi-interpenetrating nanocomposite hydrogels of PNIPAm and hectorite clay,” *React. Funct. Polym.*, vol. 71, no. 4, pp. 447–454, Apr. 2011.

[49] A. Sinha, G. Das, B. Kumar Sharma, R. Prabahan Roy, A. Kumar Pramanick, and S. Nayar, “Poly(vinyl alcohol)–hydroxyapatite biomimetic scaffold for tissue regeneration,” *Mater. Sci. Eng. C*, vol. 27, no. 1, pp. 70–74, Jan. 2007.

[50] X. Shen, L. Chen, X. Cai, T. Tong, H. Tong, and J. Hu, “A novel method for the fabrication of homogeneous hydroxyapatite/collagen nanocomposite and nanocomposite scaffold with hierarchical porosity,” *J. Mater. Sci. Mater. Med.*, vol. 22, no. 2, pp. 299–305, Feb. 2011.

[51] N. Bouropoulos, A. Stampolakis, and D. E. Mouzakis, “Dynamic Mechanical Properties of Calcium Alginate-Hydroxyapatite Nanocomposite Hydrogels,” *Sci. Adv.*

Mater., vol. 2, no. 2, pp. 239–242, Jun. 2010.

[52] M. Azami, M. J. Moosavifar, N. Baheiraei, F. Moztarzadeh, and J. Ai, "Preparation of a biomimetic nanocomposite scaffold for bone tissue engineering via mineralization of gelatin hydrogel and study of mineral transformation in simulated body fluid," *J. Biomed. Mater. Res. Part A*, vol. 100A, no. 5, pp. 1347–1355, May 2012.

[53] L. Nie *et al.*, "Physicochemical characterization and biocompatibility in vitro of biphasic calcium phosphate/polyvinyl alcohol scaffolds prepared by freeze-drying method for bone tissue engineering applications," *Colloids Surfaces B Biointerfaces*, vol. 100, pp. 169–176, Dec. 2012.

[54] B. Marelli *et al.*, "Accelerated mineralization of dense collagen-nano bioactive glass hybrid gels increases scaffold stiffness and regulates osteoblastic function," *Biomaterials*, vol. 32, no. 34, pp. 8915–8926, Dec. 2011.

[55] S. Yang, J. Wang, H. Tan, F. Zeng, and C. Liu, "Mechanically robust PEGDA–MSNs-OH nanocomposite hydrogel with hierarchical meso-macroporous structure for tissue engineering," *Soft Matter*, vol. 8, no. 34, p. 8981, 2012.

[56] K. Varaprasad, Y. M. Mohan, K. Vimala, and K. Mohana Raju, "Synthesis and characterization of hydrogel-silver nanoparticle-curcumin composites for wound dressing and antibacterial application," *J. Appl. Polym. Sci.*, vol. 121, no. 2, pp. 784–796, Jul. 2011.

[57] P. T. S. Kumar, V.-K. Lakshmanan, R. Biswas, S. V. Nair, and R. Jayakumar, "Synthesis and Biological Evaluation of Chitin Hydrogel/Nano ZnO Composite Bandage as Antibacterial Wound Dressing," *J. Biomed. Nanotechnol.*, vol. 8, no. 6, pp. 891–900, Dec. 2012.

[58] G. Sarkar, A. Dey, and S. Siddiqua, “Preparation of Wyoming bentonite nanoparticles,” *Environ. Geotech.*, p. jenge.15.00001, Feb. 2016.

[59] A. K. Gaharwar, N. A. Peppas, and A. Khademhosseini, “Nanocomposite hydrogels for biomedical applications,” *Biotechnol. Bioeng.*, vol. 111, no. 3, pp. 441–453, Mar. 2014.

[60] A. Gaharwar, A. K., Peppas, N. A., & Khademhosseini, “Nanocomposite hydrogels for biomedical applications. Biotechnology and bioengineering, 111(3), 441-453.,” vol. 18, no. 9, pp. 1199–1216, 2013.

[61] D. E. Discher, D. J. Mooney, and P. W. Zandstra, “Growth Factors, Matrices, and Forces Combine and Control Stem Cells,” *Science (80-.).*, vol. 324, no. 5935, pp. 1673–1677, Jun. 2009.

[62] M. W. Tibbitt and K. S. Anseth, “Hydrogels as extracellular matrix mimics for 3D cell culture,” *Biotechnol. Bioeng.*, vol. 103, no. 4, pp. 655–663, Jul. 2009.

[63] N. Annabi *et al.*, “25th Anniversary Article: Rational Design and Applications of Hydrogels in Regenerative Medicine,” *Adv. Mater.*, vol. 26, no. 1, pp. 85–124, Jan. 2014.

[64] S. Goenka, V. Sant, and S. Sant, “Graphene-based nanomaterials for drug delivery and tissue engineering,” *J. Control. Release*, vol. 173, pp. 75–88, Jan. 2014.

[65] G. Schexnailder, P., & Schmidt, P. Schexnailder, and G. Schmidt, “Nanocomposite polymer hydrogels.,” *Colloid Polym. Sci.*, vol. 287, no. 1, pp. 1–11, Jan. 2009.

[66] T. Thomas, J.; Peppas, N.; Sato, M.; Webster, “Nanotechnology and biomaterials.,” in *Nanomaterials handbook*, Y. Gogotsi, Ed. Boca Raton: Taylor and Francis, 2006, p. 605–636.

[67] A. M. Lowman, T. D. Dziubla, P. Bures, and N. A. Peppas, “STRUCTURAL AND DYNAMIC RESPONSE OF NEUTRAL AND INTELLIGENT NETWORKS IN BIOMEDICAL ENVIRONMENTS,” in *Molecular and cellular foundations of biomaterials.*, M. Peppas, NA.; Sefton, Ed. New York: Academic Press, 2004, pp. 75–130.

[68] N. A. Peppas, J. Z. Hilt, A. Khademhosseini, and R. Langer, “Hydrogels in Biology and Medicine: From Molecular Principles to Bionanotechnology,” *Adv. Mater.*, vol. 18, no. 11, pp. 1345–1360, Jun. 2006.

[69] C. Cha, S. R. Shin, N. Annabi, M. R. Dokmeci, and A. Khademhosseini, “Carbon-Based Nanomaterials: Multifunctional Materials for Biomedical Engineering,” *ACS Nano*, vol. 7, no. 4, pp. 2891–2897, Apr. 2013.

[70] T. Kuilla, S. Bhadra, D. Yao, N. H. Kim, S. Bose, and J. H. Lee, “Recent advances in graphene based polymer composites,” *Prog. Polym. Sci.*, vol. 35, no. 11, pp. 1350–1375, Nov. 2010.

[71] S. R. Shin *et al.*, “Cell-laden Microengineered and Mechanically Tunable Hybrid Hydrogels of Gelatin and Graphene Oxide,” *Adv. Mater.*, vol. 25, no. 44, pp. 6385–6391, Nov. 2013.

[72] C. Li and R. Mezzenga, “Functionalization of Multiwalled Carbon Nanotubes and Their pH-Responsive Hydrogels with Amyloid Fibrils,” *Langmuir*, vol. 28, no. 27, pp. 10142–10146, Jul. 2012.

[73] E. Wang, M. S. Desai, and S.-W. Lee, “Light-Controlled Graphene-Elastin Composite Hydrogel Actuators,” *Nano Lett.*, vol. 13, no. 6, pp. 2826–2830, Jun. 2013.

[74] J. Liu, C. Chen, C. He, J. Zhao, X. Yang, and H. Wang, “Synthesis of Graphene

Peroxide and Its Application in Fabricating Super Extensible and Highly Resilient Nanocomposite Hydrogels," *ACS Nano*, vol. 6, no. 9, pp. 8194–8202, Sep. 2012.

[75] E. GILLIES and J. FRECHET, "Dendrimers and dendritic polymers in drug delivery," *Drug Discov. Today*, vol. 10, no. 1, pp. 35–43, Jan. 2005.

[76] N. Joshi and M. Grinstaff, "Applications of dendrimers in tissue engineering.," *Curr. Top. Med. Chem.*, vol. 8, no. 14, pp. 1225–36, 2008.

[77] S. Zhong and L. Y. L. Yung, "Enhanced biological stability of collagen with incorporation of PAMAM dendrimer," *J. Biomed. Mater. Res. Part A*, vol. 91A, no. 1, pp. 114–122, Oct. 2009.

[78] H. Zhang *et al.*, "Hyperbranched Polyester Hydrogels with Controlled Drug Release and Cell Adhesion Properties," *Biomacromolecules*, vol. 14, no. 5, pp. 1299–1310, May 2013.

[79] J. M. Hench, L. L., & Polak, "Third-Generation Biomedical Materials," *Science (80-.).*, vol. 295, no. 5557, pp. 1014–1017, 2002.

[80] A. Hoppe, N. S. Güldal, and A. R. Boccaccini, "A review of the biological response to ionic dissolution products from bioactive glasses and glass-ceramics," *Biomaterials*, vol. 32, no. 11, pp. 2757–2774, Apr. 2011.

[81] A. K. Gaharwar, S. A. Dammu, J. M. Canter, C.-J. Wu, and G. Schmidt, "Highly Extensible, Tough, and Elastomeric Nanocomposite Hydrogels from Poly(ethylene glycol) and Hydroxyapatite Nanoparticles," *Biomacromolecules*, vol. 12, no. 5, pp. 1641–1650, May 2011.

[82] A. K. Gaharwar, C. P. Rivera, C.-J. Wu, and G. Schmidt, "Transparent, elastomeric and tough hydrogels from poly(ethylene glycol) and silicate nanoparticles," *Acta*

Biomater., vol. 7, no. 12, pp. 4139–4148, Dec. 2011.

[83] L. Bordes, P., Pollet, E., & Avérous, "Nano-biocomposites: biodegradable polyester/nanoclay systems," *Prog. Polym. Sci.*, vol. 34, no. 2, pp. 125–155, 2009.

[84] C.-J. Wu, A. K. Gaharwar, P. J. Schexnailder, and G. Schmidt, "Development of Biomedical Polymer-Silicate Nanocomposites: A Materials Science Perspective," *Materials (Basel).*, vol. 3, no. 5, pp. 2986–3005, Apr. 2010.

[85] T. Dvir *et al.*, "Nanowired three-dimensional cardiac patches," *Nat. Nanotechnol.*, vol. 6, no. 11, pp. 720–725, Sep. 2011.

[86] A. K. Gaharwar, J. E. Wong, D. Müller-Schulte, D. Bahadur, and W. Richtering, "Magnetic Nanoparticles Encapsulated Within a Thermoresponsive Polymer," *J. Nanosci. Nanotechnol.*, vol. 9, no. 9, pp. 5355–5361, Sep. 2009.

[87] R. L. Price, L. G. Gutwein, L. Kaledin, F. Tepper, and T. J. Webster, "Osteoblast function on nanophase alumina materials: Influence of chemistry, phase, and topography," *J. Biomed. Mater. Res.*, vol. 67A, no. 4, pp. 1284–1293, Dec. 2003.

[88] T. J. Webster, R. W. Siegel, and R. Bizios, "Nanoceramic surface roughness enhances osteoblast and osteoclast functions for improved orthopaedic/dental implant efficacy," *Scr. Mater.*, vol. 44, no. 8–9, pp. 1639–1642, May 2001.

[89] A. Khademhosseini, J. P. Vacanti, and R. Langer, "Progress in Tissue Engineering," *Sci. Am.*, vol. 300, no. 5, pp. 64–71, May 2009.

[90] K. Yue *et al.*, "Synthesis, properties, and biomedical applications of gelatin methacryloyl (GelMA) hydrogels," *Biomaterials*, vol. 73, pp. 254–271, Dec. 2015.

[91] J. K. Carrow and A. K. Gaharwar, "Bioinspired Polymeric Nanocomposites for Regenerative Medicine," *Macromol. Chem. Phys.*, vol. 216, no. 3, pp. 248–264, Feb.

2015.

[92] J. D. Ferry and H. S. Myers, “Viscoelastic Properties of Polymers,” *J. Electrochem. Soc.*, vol. 108, no. 7, p. 142C, 1961.

[93] J. Thiele, Y. Ma, S. M. C. Bruekers, S. Ma, and W. T. S. Huck, “25th Anniversary Article: Designer Hydrogels for Cell Cultures: A Materials Selection Guide,” *Adv. Mater.*, vol. 26, no. 1, pp. 125–148, Jan. 2014.

[94] M. B. Liu, Y., & Chan-Park, “A biomimetic hydrogel based on methacrylated dextran-graft-lysine and gelatin for 3D smooth muscle cell culture,” *Biomaterials*, vol. 31, no. 6, pp. 1158–1170, 2010.

[95] S. Gorgieva and V. Kokol, “Collagen- vs. Gelatine-Based Biomaterials and Their Biocompatibility: Review and Perspectives,” in *Biomaterials Applications for Nanomedicine*, InTech, 2011.

[96] J. W. Nichol, S. Koshy, H. Bae, C. M. Hwang, and A. Khademhosseini, “Cell-laden microengineered gelatin methacrylate hydrogels,” vol. 31, no. 21, pp. 5536–5544, 2011.

[97] J. A. Benton, C. A. DeForest, V. Vivekanandan, and K. S. Anseth, “Photocrosslinking of Gelatin Macromers to Synthesize Porous Hydrogels That Promote Valvular Interstitial Cell Function,” *Tissue Eng. Part A*, vol. 15, no. 11, pp. 3221–3230, Nov. 2009.

[98] H. Aubin *et al.*, “Directed 3D cell alignment and elongation in microengineered hydrogels,” *Biomaterials*, vol. 31, no. 27, pp. 6941–6951, Sep. 2010.

[99] a I. Van Den Bulcke, B. Bogdanov, N. De Rooze, E. H. Schacht, M. Cornelissen, and H. Berghmans, “Structural and rheological properties of methacrylamide modified

gelatin hydrogels.," *Biomacromolecules*, vol. 1, no. 1, pp. 31–38, 2000.

[100] E. Hoch, C. Schuh, T. Hirth, G. E. M. Tovar, and K. Borchers, "Stiff gelatin hydrogels can be photo-chemically synthesized from low viscous gelatin solutions using molecularly functionalized gelatin with a high degree of methacrylation," *J. Mater. Sci. Mater. Med.*, vol. 23, no. 11, pp. 2607–2617, Nov. 2012.

[101] B. D. Fairbanks, M. P. Schwartz, C. N. Bowman, and K. S. Anseth, "Photoinitiated polymerization of PEG-diacrylate with lithium phenyl-2,4,6-trimethylbenzoylphosphinate: polymerization rate and cytocompatibility," *Biomaterials*, vol. 30, no. 35, pp. 6702–6707, Dec. 2009.

[102] S. T. Koshy, T. C. Ferrante, S. A. Lewin, and D. J. Mooney, "Injectable, porous, and cell-responsive gelatin cryogels," *Biomaterials*, vol. 35, no. 8, pp. 2477–2487, Mar. 2014.

[103] S. Van Vlierberghe, P. Dubruel, and E. Schacht, "Effect of Cryogenic Treatment on the Rheological Properties of Gelatin Hydrogels," *J. Bioact. Compat. Polym.*, vol. 25, no. 5, pp. 498–512, Sep. 2010.

[104] Y. Lee, J. M. Lee, P.-K. Bae, I. Y. Chung, B. H. Chung, and B. G. Chung, "Photo-crosslinkable hydrogel-based 3D microfluidic culture device," *Electrophoresis*, vol. 36, no. 7–8, pp. 994–1001, Apr. 2015.

[105] Y.-C. Chen *et al.*, "Functional Human Vascular Network Generated in Photocrosslinkable Gelatin Methacrylate Hydrogels," *Adv. Funct. Mater.*, vol. 22, no. 10, pp. 2027–2039, May 2012.

[106] P. Dubruel *et al.*, "Porous Gelatin Hydrogels: 2. In Vitro Cell Interaction Study," *Biomacromolecules*, vol. 8, no. 2, pp. 338–344, Feb. 2007.

[107] S. R. Shin *et al.*, “Carbon-Nanotube-Embedded Hydrogel Sheets for Engineering Cardiac Constructs and Bioactuators,” *ACS Nano*, vol. 7, no. 3, pp. 2369–2380, Mar. 2013.

[108] A. Shin, H., Olsen, B. D., & Khademhosseini, “The mechanical properties and cytotoxicity of cell-laden double-network hydrogels based on photocrosslinkable gelatin and gellan gum biomacromolecules.,” *Biomaterials*, vol. 18, no. 9, pp. 1199–1216, 2013.

[109] S. R. Shin *et al.*, “A Bioactive Carbon Nanotube-Based Ink for Printing 2D and 3D Flexible Electronics,” *Adv. Mater.*, vol. 28, no. 17, pp. 3280–3289, May 2016.

[110] P.-C. Ma, N. A. Siddiqui, G. Marom, and J.-K. Kim, “Dispersion and functionalization of carbon nanotubes for polymer-based nanocomposites: A review,” *Compos. Part A Appl. Sci. Manuf.*, vol. 41, no. 10, pp. 1345–1367, Oct. 2010.

[111] S. J. V Frankland, a Caglar, D. W. Brenner, and M. Griebel, “Molecular Simulation of the Influence of Chemical Cross-Links on the Shear Strength of Carbon Nanotube - Polymer Interfaces,” *J. Phys. Chem. B*, vol. 106, pp. 3046–3048, 2002.

[112] C. Cha *et al.*, “Controlling Mechanical Properties of Cell-Laden Hydrogels by Covalent Incorporation of Graphene Oxide,” *Small*, vol. 10, no. 3, pp. 514–523, Feb. 2014.

[113] M. Paul, A., Hasan, A., Al Kindi, H., Gaharwar, A.K., Rao, V.T.S., Nikkhah, “Injectable graphene oxide/hydrogel-based angiogenic gene delivery system for vasculogenesis and cardiac repair,” *ACS Nano*, no. 8, p. 8050e8062, 2014.

[114] H. Ahadian, S., Estili, M., Surya, V.J., Ramon-Azcon, J., Liang, X., Shiku, “Facile and green production of aqueous graphene dispersions for biomedical applications,”

Nanoscale, vol. 7, p. 6436e6443, 2015.

[115] M. Biondi, A. Borzacchiello, L. Mayol, and L. Ambrosio, "Nanoparticle-Integrated Hydrogels as Multifunctional Composite Materials for Biomedical Applications," *Gels*, vol. 1, no. 2, pp. 162–178, Oct. 2015.

[116] J. R. Xavier *et al.*, "Bioactive Nanoengineered Hydrogels for Bone Tissue Engineering: A Growth-Factor-Free Approach," *ACS Nano*, vol. 9, no. 3, pp. 3109–3118, Mar. 2015.

[117] A. K. Gaharwar *et al.*, "Bioactive Silicate Nanoplatelets for Osteogenic Differentiation of Human Mesenchymal Stem Cells," *Adv. Mater.*, vol. 25, no. 24, pp. 3329–3336, 2013.

[118] A. Paul *et al.*, "Nanoengineered biomimetic hydrogels for guiding human stem cell osteogenesis in three dimensional microenvironments," *J. Mater. Chem. B*, vol. 4, no. 20, pp. 3544–3554, 2016.

[119] A. K. Gaharwar *et al.*, "Shear-Thinning Nanocomposite Hydrogels for the Treatment of Hemorrhage," *ACS Nano*, vol. 8, no. 10, pp. 9833–9842, Oct. 2014.

[120] S. Ahadian *et al.*, "Hybrid hydrogels containing vertically aligned carbon nanotubes with anisotropic electrical conductivity for muscle myofiber fabrication," *Sci. Rep.*, vol. 4, no. 1, p. 4271, May 2015.

[121] W. Heo, D.N., Ko, W.-K., Bae, M.S., Lee, J.B., Lee, D.-W., Byun, "Enhanced bone regeneration with a gold nanoparticle-hydrogel complex," *J. Mater Chem. B*, vol. 2, p. 1584e1593., 2014.

[122] C. Zhou, L., Tan, G., Tan, Y., Wang, H., Liao, J., Ning, "Biomimetic mineralization of anionic gelatin hydrogels: effect of degree of methacrylation," *RSC Adv*, vol. 4, p.

21997e22008., 2014.

[123] J. Tan, G., Zhou, L., Ning, C., Tan, Y., Ni, G., Liao, "Biomimetically-mineralized composite coatings on titanium functionalized with gelatin methacrylate hydrogels," *Appl. Surf. Sci.*, vol. 279, p. 293e299, 2013.

[124] A. C. Balazs, T. Emrick, and T. P. Russell, "Nanoparticle Polymer Composites: Where Two Small Worlds Meet," *Science (80-.).*, vol. 314, no. 5802, pp. 1107–1110, Nov. 2006.

[125] F. Caruso, "Nanoengineering of Particle Surfaces," *Adv. Mater.*, vol. 13, no. 1, pp. 11–22, Jan. 2001.

[126] C. García-Astrain *et al.*, "Biocompatible Hydrogel Nanocomposite with Covalently Embedded Silver Nanoparticles," *Biomacromolecules*, vol. 16, no. 4, pp. 1301–1310, Apr. 2015.

[127] D. Pasqui, A. Atrei, G. Giani, M. De Cagna, and R. Barbucci, "Metal oxide nanoparticles as cross-linkers in polymeric hybrid hydrogels," *Mater. Lett.*, vol. 65, no. 2, pp. 392–395, Jan. 2011.

[128] J. Tan, G., Zhou, L., Ning, C., Tan, Y., Ni, G., Liao *et al.*, "Biomimetically-mineralized composite coatings on titanium functionalized with gelatin methacrylate hydrogels," *Appl. Surf. Sci.*, vol. 279, pp. 293–299, Aug. 2013.

[129] G. X. Tan, Y. Tan, C. Y. Ning, L. Zhang, L. Zhou, and H. Wang, "Protein Adsorption on Titanium Surface Functionalized with Bioactive Gelatin Methacrylate Hydrogel Coating," *Adv. Mater. Res.*, vol. 936, pp. 663–668, Jun. 2014.

[130] S. Si, R. Zhou, Z. Xing, H. Xu, Y. Cai, and Q. Zhang, "A study of hybrid organic/inorganic hydrogel films based on in situ-generated TiO2 nanoparticles and

methacrylated gelatin," *Fibers Polym.*, vol. 14, no. 6, pp. 982–989, Jun. 2013.

[131] O. R. Dawson JI, "Clay: New opportunities for tissue regeneration and biomaterial design.," *Adv Mater*, vol. 25, no. 30, p. 4069–4086., 2013.

[132] J. I. Dawson and R. O. C. Oreffo, "Clay: New Opportunities for Tissue Regeneration and Biomaterial Design," *Adv. Mater.*, vol. 25, no. 30, pp. 4069–4086, Aug. 2013.

[133] A. Khademhosseini, P. J. Vacanti, and R. Langer, "Progress in tissue engineering," *Sci. Am.*, vol. 300, no. 5, pp. 64–71, 2009.

[134] A. M. Kloxin, C. J. Kloxin, C. N. Bowman, and K. S. Anseth, "Mechanical Properties of Cellularly Responsive Hydrogels and Their Experimental Determination," *Adv. Mater.*, vol. 22, no. 31, pp. 3484–3494, May 2010.

[135] K. S. Novoselov, "Electric Field Effect in Atomically Thin Carbon Films," *Science (80-.).*, vol. 306, no. 5696, pp. 666–669, Oct. 2004.

[136] R. J. Young, I. A. Kinloch, L. Gong, and K. S. Novoselov, "The mechanics of graphene nanocomposites: A review," *Compos. Sci. Technol.*, vol. 72, no. 12, pp. 1459–1476, Jul. 2012.

[137] D. Chimene, D. L. Alge, and A. K. Gaharwar, "Two-Dimensional Nanomaterials for Biomedical Applications: Emerging Trends and Future Prospects," *Adv. Mater.*, vol. 27, no. 45, pp. 7261–7284, Dec. 2015.

[138] X. Zhuang, Y. Mai, D. Wu, F. Zhang, and X. Feng, "Two-Dimensional Soft Nanomaterials: A Fascinating World of Materials," *Adv. Mater.*, vol. 27, no. 3, pp. 403–427, Jan. 2015.

[139] K. L. Aillon, Y. Xie, N. El-Gendy, C. J. Berkland, and M. L. Forrest, "Effects of nanomaterial physicochemical properties on in vivo toxicity," *Adv. Drug Deliv. Rev.*,

vol. 61, no. 6, pp. 457–466, Jun. 2009.

[140] K. S. Katti, D. R. Katti, and R. Dash, “Synthesis and characterization of a novel chitosan/montmorillonite/hydroxyapatite nanocomposite for bone tissue engineering,” *Biomed. Mater.*, vol. 3, no. 3, p. 34122, Sep. 2008.

[141] J. P. Zheng, C. Z. Wang, X. X. Wang, H. Y. Wang, H. Zhuang, and K. De Yao, “Preparation of biomimetic three-dimensional gelatin/montmorillonite–chitosan scaffold for tissue engineering,” *React. Funct. Polym.*, vol. 67, no. 9, pp. 780–788, Sep. 2007.

[142] A. A. Haroun, A. Gamal-Eldeen, and D. R. K. Harding, “Preparation, characterization and in vitro biological study of biomimetic three-dimensional gelatin–montmorillonite/cellulose scaffold for tissue engineering,” *J. Mater. Sci. Mater. Med.*, vol. 20, no. 12, pp. 2527–2540, Dec. 2009.

[143] M. Swetha, K. Sahithi, A. Moorthi, N. Srinivasan, K. Ramasamy, and N. Selvamurugan, “Biocomposites containing natural polymers and hydroxyapatite for bone tissue engineering,” *Int. J. Biol. Macromol.*, vol. 47, no. 1, pp. 1–4, Jul. 2010.

[144] P. Kerativitayanan, J. K. Carrow, and A. K. Gaharwar, “Nanomaterials for Engineering Stem Cell Responses,” *Adv. Healthc. Mater.*, vol. 4, no. 11, pp. 1600–1627, Aug. 2015.

[145] Z. Mũnoz, H. Shih, and C.-C. Lin, “Gelatin hydrogels formed by orthogonal thiol–norbornene photochemistry for cell encapsulation,” *Biomater. Sci.*, vol. 2, no. 8, pp. 1063–1072, 2014.

[146] A. J. García, “Get a grip: integrins in cell–biomaterial interactions,” *Biomaterials*, vol. 26, no. 36, pp. 7525–7529, Dec. 2005.

[147] B. M. Das, *Advanced Soil Mechanics*. CRC Press, 2013.

[148] D. A. Dixon, “Sodium bentonites of Canada, the United States and Mexico: sources, reserves and properties,” in *Engineering materials for waste isolation. Engineering material division special publication*, 1994, pp. 37–65.

[149] N. Latifi, A. S. A. Rashid, S. Siddiqua, and S. Horpibulsuk, “Micro-structural analysis of strength development in low- and high swelling clays stabilized with magnesium chloride solution — A green soil stabilizer,” *Appl. Clay Sci.*, vol. 118, pp. 195–206, Dec. 2015.

[150] M. Catauro, F. Bollino, A. Dell’Era, and S. V. Ciprioti, “Pure Al 2 O 3 ·2SiO 2 synthesized via a sol-gel technique as a raw material to replace metakaolin: Chemical and structural characterization and thermal behavior,” *Ceram. Int.*, vol. 42, no. 14, pp. 16303–16309, Nov. 2016.

[151] N. Annabi *et al.*, “Controlling the Porosity and Microarchitecture of Hydrogels for Tissue Engineering,” *Tissue Eng. Part B Rev.*, vol. 16, no. 4, pp. 371–383, Aug. 2010.

[152] Y. Du, E. Lo, S. Ali, and A. Khademhosseini, “Directed assembly of cell-laden microgels for fabrication of 3D tissue constructs,” *Proc. Natl. Acad. Sci.*, vol. 105, no. 28, pp. 9522–9527, Jul. 2008.

[153] Q. Wang, R. Hou, Y. Cheng, and J. Fu, “Super-tough double-network hydrogels reinforced by covalently compositing with silica-nanoparticles,” *Soft Matter*, vol. 8, no. 22, p. 6048, 2012.

[154] R. A. Hule and D. J. Pochan, “Polymer Nanocomposites for Biomedical Applications,” *MRS Bull.*, vol. 32, no. 4, pp. 354–358, Apr. 2007.

[155] Z. Wang, Z. Tian, F. Menard, and K. Kim, “Comparative study of gelatin methacrylate

hydrogels from different sources for biofabrication applications," *Biofabrication*, vol. 9, no. 4, p. 44101, Aug. 2017.

[156] C. A. Durst, M. P. Cuchiara, E. G. Mansfield, J. L. West, and K. J. Grande-Allen, "Flexural characterization of cell encapsulated PEGDA hydrogels with applications for tissue engineered heart valves," *Acta Biomater.*, vol. 7, no. 6, pp. 2467–2476, Jun. 2011.

[157] H.-W. Kang, S. J. Lee, I. K. Ko, C. Kengla, J. J. Yoo, and A. Atala, "A 3D bioprinting system to produce human-scale tissue constructs with structural integrity," *Nat. Biotechnol.*, vol. 34, no. 3, pp. 312–319, Feb. 2016.

[158] Y. Du, M. Ghodousi, E. Lo, M. K. Vidula, O. Emiroglu, and A. Khademhosseini, "Surface-directed assembly of cell-laden microgels," *Biotechnol. Bioeng.*, vol. 105, no. 3, pp. 655–662, Feb. 2010.

[159] Y. Ke, L. L. Ong, W. M. Shih, and P. Yin, "Three-Dimensional Structures Self-Assembled from DNA Bricks," *Science (80-.).*, vol. 338, no. 6111, pp. 1177–1183, Nov. 2012.

[160] B. Wei, M. Dai, and P. Yin, "Complex shapes self-assembled from single-stranded DNA tiles," *Nature*, vol. 485, no. 7400, pp. 623–626, May 2012.

[161] C. Colosi *et al.*, "Microfluidic Bioprinting of Heterogeneous 3D Tissue Constructs Using Low-Viscosity Bioink," *Adv. Mater.*, vol. 28, no. 4, pp. 677–684, Jan. 2016.